*Marked Revised Manuscript
Click here to view linked References

Highly Conductive PEDOT Films with Enhanced Catalytic Activity for Dye-Sensitized Solar Cells

Mojgan Kouhnavard[a], Diao Yifan[b], Julio M. D' Arcy[b,c], Rohan Mishra[d], Pratim Biswas[a]*

[a]Aerosol and Air Quality Research Laboratory
Department of Energy, Environmental and Chemical Engineering
Washington University in St. Louis
One Brookings Drive
St. Louis 63130, Missouri, United States

[b]Institute of Materials Science & Engineering,
[c]Department of Chemistry
[d]Department of Mechanical Engineering & Material Science

Revised Version of SE-D-20-01655
Submitted to
Solar Energy

July 23, 2020

*To Whom Correspondence Should be Addressed: pbiswas@wustl.edu

Abstract

Low-cost poly (3,4 ethylenedioxythiophene) (PEDOT) films with a high electronic conductivity of 1021 S/cm were successfully deposited via iron oxide-based vapor-phase polymerization and used as a counter electrode (CE) in dye-sensitized solar cells for the first time. Reaching a high efficiency of 8.4%, the CE showed outstanding catalytic activity in iodine/triiodide (I^-/I_3^-) reduction, with a six times lower charge transfer resistance than a standard Pt CE. Combining low cost, easy fabrication, and high electro-catalytic activity, our PEDOT films are a promising replacement for expensive platinum CEs. This efficiency is one of the highest reported among the PEDOT-based DSSC.

Keywords: Dye-sensitized solar cell, Low-cost counter electrode, PEDOT, Vapor phase polymerization, Electrocatalytic activity, Conversion efficiency.

1. Introduction

Dye-sensitized solar cells (DSSCs) are low cost and simple to make, and they have a relatively high conversion efficiency of ~12% (Grätzel, 2009). Generally, DSSCs consist of a porous TiO_2 electrode sensitized with an absorbing layer, an electrolyte, and a platinum (Pt) counter electrode (CE). In DSSCs, CE are used to reduce an oxidized redox couple, to collect and transmit the electrons back into the cell, and to reflect unabsorbed light back to the cell, enhancing the utilization of solar energy. To ensure an efficient redox reaction in the electrolyte, an ideal CE should possess high conductivity, high electrochemical and mechanical stability, and high catalytic activity. Pt, because of its high conductivity and excellent catalytic activity toward I_3^- (iodide) reduction, is the most nearly ideal CE in DSSC (Briscoe and Dunn, 2016).

However, large-scale use of Pt is limited by its low stability in the redox electrolyte, as well as by its high cost and rarity. An alternative CE is highly desirable, one with low-cost fabrication, easy scalability, high photocorrosion stability, and relatively high conversion efficiency. To this end, many works have carried out to substitute Pt with suitable alternatives, such as carbonaceous material (Kouhnavard et al., 2016, 2015; Ren et al., 2015; Zheng et al., 2014), metal oxide (Guo et al., 2015; Ahn and Manthiram, 2016; Zhang et al., n.d.), and polymers (Ghani et al., 2015; Lu et al., 2015). Among these alternatives, polymers are advantageous for their low cost and high catalytic activity (Jeon et al., 2011; Park and Jang, 2016; Tai et al., 2011; Tang et al., 2012; Zhou et al., 2018). Polypyrrole (PPy), polyaniline (PANI) (Tai et al., 2011), and poly (3,4 ethylenedioxythiophene) (PEDOT) (Kim et al., 2018) are commonly used as conductive polymer CEs in DSSC or as hole transporting materials in perovskite solar cells (Liu et al., 2020; M. Wang et al., 2018; Wang et al., 2019; Zeng et al., 2017; Zhou et al., 2019). Amongst them, PEDOT is attractive as it possesses the highest transparency, stability, and catalytic activity (Zhang et al., 2012). Its conductivity, 300-600 $S.cm^{-1}$, is also much higher than those of PANI (~5 S/cm) and PPy (~50 S/cm) (Kim et al., n.d.; Ha et al., 2004; See et al., 2010; Wei et al., 2014;(Hou et al., 2019; Wu et al., 2017). However, the existing conductivity can be increased by various methods, such as by annealing at elevated temperatures (Lee et al., 2014a), acid treatment (Lee et al., 2014b), adding co-solvents (Wei et al., 2013; G. T. Yue et al., 2013), and doping to enhance the crystallization of the films (Gueye et al., 2016; Rudd et al., 2018). Zhang et al. used cyclic voltammetry (a three-electrode system) to deposit three different CEs with different carbon doped polymers to fabricate a DSSC (Zhang et al., 2012) with C160 ruthenium dye. PEDOT+ carbon black (C) exhibited the highest efficiency, 7.6%, compared to PANI+C and PPY+C with efficiencies of ~5.2%, prepared under the same experimental condition.

Typically, PEDOT films are generated via electrochemical polymerization under constant voltage or constant current, which results in low electrical conductivity (Trevisan et al., 2011; Lin et al., 2016; Zhang et al., 2012). For example, Li et al.(2017) report a PEDOT/rGO composite film possessing a conversion efficiency of 7.115%; however, their electrochemical method requires a potentiostat, a three-electrode system, and refined control of voltage, all of which decrease the film's reproducibility. Alternatively, toluenesulfonate, ClO, poly(styrenesulfonate) (PSS)(G. T. Yue et al., 2013), TsO ; Saito et al., 2002) and polyoxometalate (POM)) are frequently employed as dopants to increase the solubility or electrical conductivity of PEDOT. The water solubility and simple fabrication process of PEDOT:PSS make it an interesting industrial polymer. G. T. Yue et al. (2013) deposited PEDOT:PSS/carbon on an fluorine doped tin oxide (FTO) glass with a scratch method under infrared light irradiation and used it as a CE for DSSC. They achieved the highest reported conductivity for a PEDOT:PSS/carbon electrode, 173 S/cm, and a resulting cell efficiency of 7.6%.

Another synthesis approach is oxidative vapor phase polymerization (VPP) using various oxidants such as $MoCl_5$ (Han Kim et al., 2015), $Fe(ClO_4)_3$ (Anothumakkool et al., 2016), and $FeCl_3$ (Kim et al., 2003; Jo et al., 2012; X. Wang et al., 2018). However, these oxidants require fabrication in a controlled environment (Winther-Jensen and West, 2004a). Bjorn et al. synthesized a PEDOT film via chemical vapor deposition (CVD) by controlling the humidity and pressure, achieving a PEDOT conductivity of only 1000 S/cm (Winther-Jensen and West, 2004b).

It is worth noting that single-crystal PEDOT has a reported electrical conductivity as high as 8797 S/cm, which is significantly higher than that observed in the thin films desired for electronic devices (White et al., 2013). These limitations highlight the urgency of advancing current PEDOT film fabrication protocols so that they are facile, cheap, and yield high conductivity. Several methods have been proposed, mainly using VPP with $FeCl_3$ as an oxidant, but to the best of our knowledge our method has never been applied in DSSC. Herein, we present a low-cost approach for engineering superior quality PEDOT films on FTO glass, using iron oxide (rust) -based vapor-phase polymerization (RVPP) (Diao et al., 2019). We used Fe_2O_3 (rust) as an oxidant because it is the cheapest and most thermodynamically stable Fe phase. The electronic conductivity of the films are reported. The film as synthesized was used as a CE in a Pt-free DSSC.

2. Experimental:

2.1 Counter electrode preparation:

FTO glass substrates (TEC™ 7) were purchased from MSE supplies LLC, USA. First, the FTO glass substrates were washed via ultrasonic baths in acetone and then in isopropyl alcohol for 20 minutes, each. Then they were treated under UV-ozone for 30 minutes to remove remaining organic impurities.

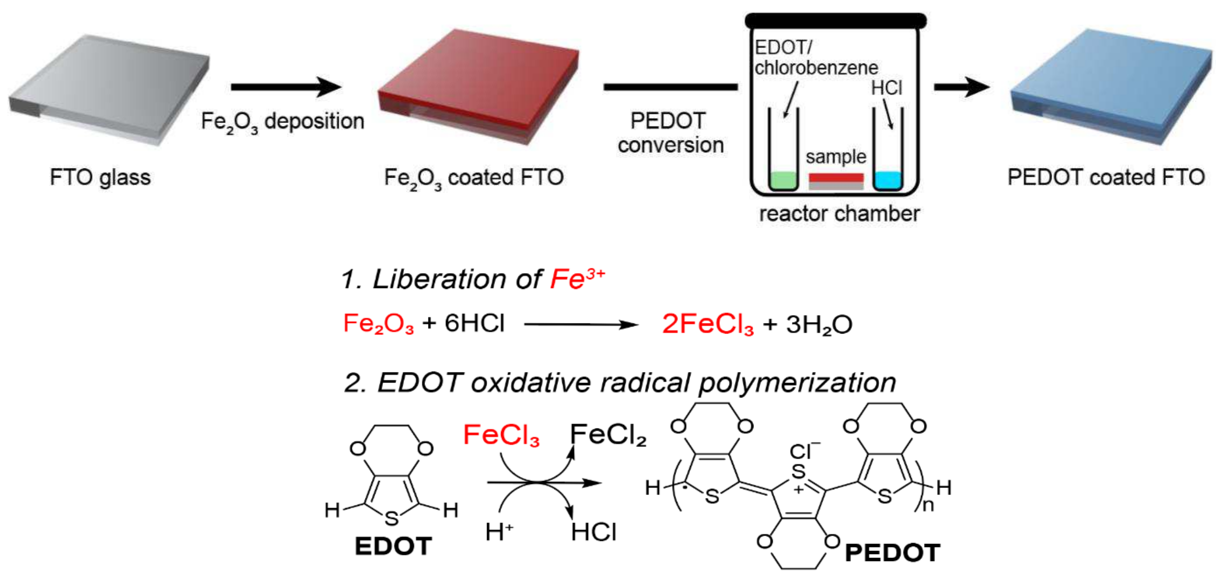

Fig. 1. Schematic of PEDOT/FTO fabrication and its mechanism for the liberation of Fe^{3+} and formation of PEDOT via step-growth polymerization.

Next, a solid-oxidant precursor, 20-nm thick Fe_2O_3, was sputtered over the FTO via physical vapor deposition (Kurt J. Lesker PVD 75 RF and DC). A glass reactor was loaded with the Fe_2O_3-coated FTO, 40 µL of HCl, and 200 µL of a 0.674 M EDOT solution in chlorobenzene, then sealed and heated in an oven at 140 °C for 1.5 hr. The samples were purified via 6 M H_2SO_4 overnight to remove iron impurities. (Fig. 1). The sputtered α-Fe_2O_3 was used as a ferric ioncontaining solid-state oxidant-precursor to induce dissolution, liberation of ferric ions, and Fe^{3+} hydrolysis concomitant with oxidative radical polymerization.

2.2 Solar cell materials and device fabrication process

A working electrode was made of two layers of screen printed TiO_2 nanoparticles (transparent TiO_2 and a reflective TiO_2) treated with $TiCl_4$, resulting in an overall thickness of 12-16 µm. The final TiO_2 film was then annealed at 450 °C for 30 minutes before immersing it in a dye solution of N719, 20 mg/mL in ethanol. The working electrode was soaked in the dye solution after being cooled to 70 °C. After 12 hours, it was rinsed with ethanol, and dried. The Pt electrode was made by drop casting Plastisol T/SP precursor solution on the FTO glass and was used as the reference CE. Finally, both the CE and the working electrode were clipped together and filled with Iodolyte AN-50 (Solaronix, Aus) electrolyte. Then the cell was tested under ambient conditions (30-50% relative humidity) and AM1.5 illumination.

2.3 Characterization:

To investigate their crystal structure, PEDOT films were characterized with an X-ray diffractometer (XRD, Bruker D8 ADVANCE, Bruker, USA) configured with a 1.5418 Å Cu X-ray operating at 40 kV. Field-emission scanning electron microscopy (FE-SEM, Nova NanoSEM 230) also used to investigate the surface morphology of the PEDOT films on the FTO substrate. Four-point probe measurements were carried out using a Keithley 2450 SourceMeter with a Signatone SP4 four-point probe head. Cyclic voltammetry (CV) analysis and electro impedance spectroscopy (EIS) were conducted using a BioLogic VMP3 multi-potentiostat. CV was carried out with three-electrode configurations at a scan rate of 50 mV/s. Ag/AgCl (3 M KCl) was used as a reference electrode, Pt and PEDOT films were the working electrodes, and Pt wire was the CE, in an acetonitrile solution containing LiI (10 mM), I_2 (1mM), and $LiClO_4$ (0.1M) as supporting electrolytes. The surface area of the CEs was 1 cm^2. EIS characterization was carried out using a symmetric cell, which consisted of two same CEs facing each other (Pt-Pt and PEDOT-PEDOT), and the space between the CEs was filled with the same electrolyte as used in full DSSC. EIS was operated at open circuit voltage using an ac perturbation of 10 mV and a frequency range 100 kHz to 0.1 Hz. The spectra were then analyzed by fitting the arc observed at the highest frequency in Nyquist plots to the equivalent circuit, which contained the series resistance (R_S), charge transfer resistance (R_{CT}), and constant phase element (CPE).

3. Results and Discussion

3.1. Morphology and crystal structure of PEDOT CE

Fig. 2a shows a SEM image of a PEDOT film on an FTO glass substrate. The film consists of bundles and nanofibers that result from, respectively, the removal of iron crystals formed during iron hydrolysis and EDOT oxidative radical polymerization through RVPP.(H. Wang et al., 2018; Diao et al., 2019). Fig. 2b shows XRD patterns of the same PEDOT film on a glass substrate. Three characteristic peaks are centered at 6.5°, 13.0°, and 26.5°. The wide diffraction peak at 26.5° corresponds to the (020) reflection, which is due to π−π stacking, whereas the sharp peaks at 6.5° and 13.0° are assigned to (200) and (100) reflections, respectively, and correspond to lateral chain packing. A four-point probe conductivity measurement was also carried out and demonstrated an exceedingly high conductivity of 1120 S/cm, mainly the result of the PEDOT crystal structure and its high charge carrier concentration (Ugur et al., 2015). The thickness of the PEDOT film is around 200 nm, measured using a profilometer (Fig. S1).

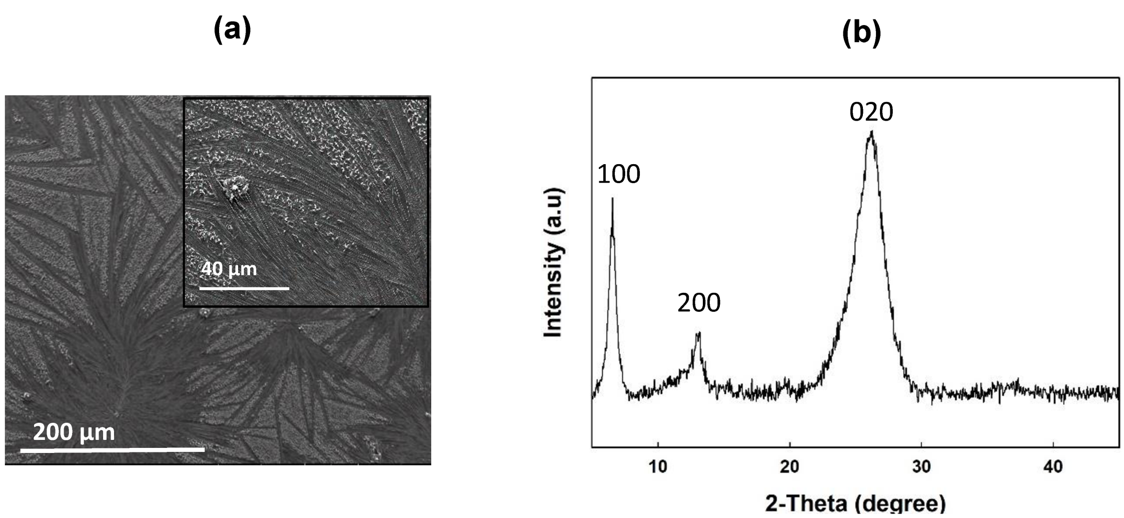

Fig. 2 (a) SEM image of a PEDOT film on an FTO substrate (b) XRD spectra of a PEDOT film on a glass substrate.

3.2. Electrochemical properties of PEDOT CE

The electrocatalytic activities of the PEDOT CEs were evaluated by CV to quantify the electrocatalytic activities of the CEs in the electrolyte. The Pt CE was also prepared under the same experimental conditions for comparison. In CV analysis, the oxidation of I^- and the reduction of I_3^- are the major redox reactions, corresponding to the anodic (J_{pa}) and cathodic (J_{pc}) peak current densities, respectively. These peaks are labeled in Fig. 3, which shows the CV diagrams of PEDOT and Pt CEs. J_{pa} in CV is not important to us, because the main role of a CE is to prompt the reduction of I_3^- in the DSSC. Therefore, J_{pc} and the potential difference between the J_{pa} and J_{pc} (ΔE_{pp}) are our focuses in this graph. The very high J_{pc} value of PEDOT (6.0 mA/cm^2), compared to Pt electrode with a J_{pc} of 2.7 mA/cm^2, indicates the outstanding electrocatalytic activity of the PEDOT CE in the I_3^- reduction reaction (Prigodin and Epstein, 2001). The lower peak potential separation (ΔE_{pp}) for PEDOT film also shows a quicker reaction rate for the reduction of I_3^- to I^-. Both factors together result in higher values of the short-current density (J_{SC}) and fill factor (FF) in a complete cell, owing to higher charge transfer through the electrolyte and CE interface and a lower recombination rate at the electrolyte and working electrode interface, respectively.

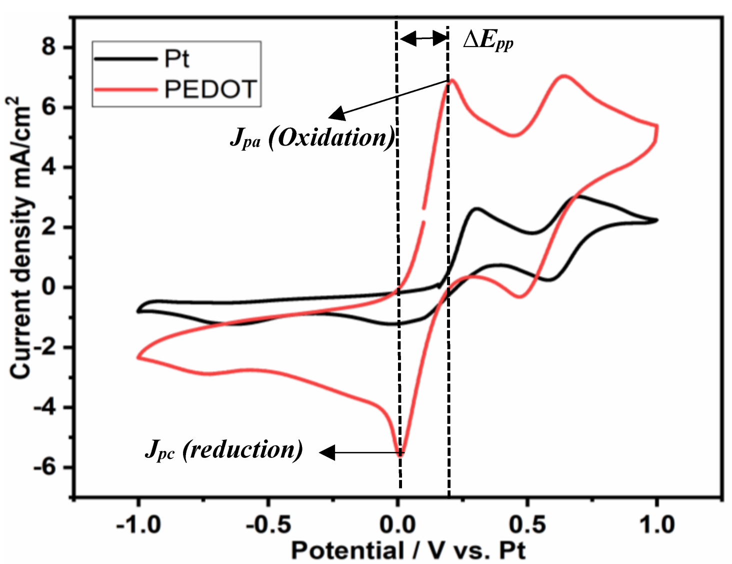

Fig. 3. Cyclic voltammograms of Pt and PEDOT film as counter electrodes for DSSC at a scan rate of 50 mV/s.

Fig. 4a shows 30 successive scan cycles of the PEDOT CE at a fixed scan rate. The peak current densities change with the change in scan rate, while the potential remains unchanged, which indicates that the PEDOT film possesses good chemical stability and is firmly coated on the FTO substrate (G. Yue et al., 2013). Fig. 4b displays the CVs of the PEDOT at scan rates ranging from 25mV/s to 200 mV/s. As the scan rate is increased, the cathodic and anodic peaks slowly shift in the negative and positive directions, respectively. In addition, Fig. 4c shows a linear relationship between the current density and the square root of the scan rate, indicating that the reduction reaction of the redox couples at the PEDOT CE is controlled by ionic diffusion of iodide species within the electrolyte, and accordingly follows the Randles-Sevcik equation (Sun et al., n.d.; Yue et al., 2014).

We further investigated the electrochemical features of the CEs by EIS measurements in a symmetric cell in which the iodine electrolyte solution was filled in the interspaces of two facing identical CEs to eliminate the effect of the photoanode. A fixed electrode area of 1 cm^2 was used for these measurements. Fig. 4d shows the Nyquist plot of the real impedance, Z', on the x-axis versus the imaginary impedance, -Z'', on the y-axis for Pt and PEDOT cells . The intercept of the high frequency (100 kHz) semicircle on the x-axis represents the series resistance (R_s). The diameter of the high-frequency semicircle equals both the charge transfer resistance (R_{ct}) at the CE/electrolyte interface as well as the redox species (I^-/I_3^-) diffusion resistance (Z_w) in the electrolyte. The equivalent RC circuit model is also given in inset (d) of Fig. 4 and was used to obtain the EIS parameters (R_S, R_{ct}, Z_w) by fitting the impedance spectra to the equivalent model.

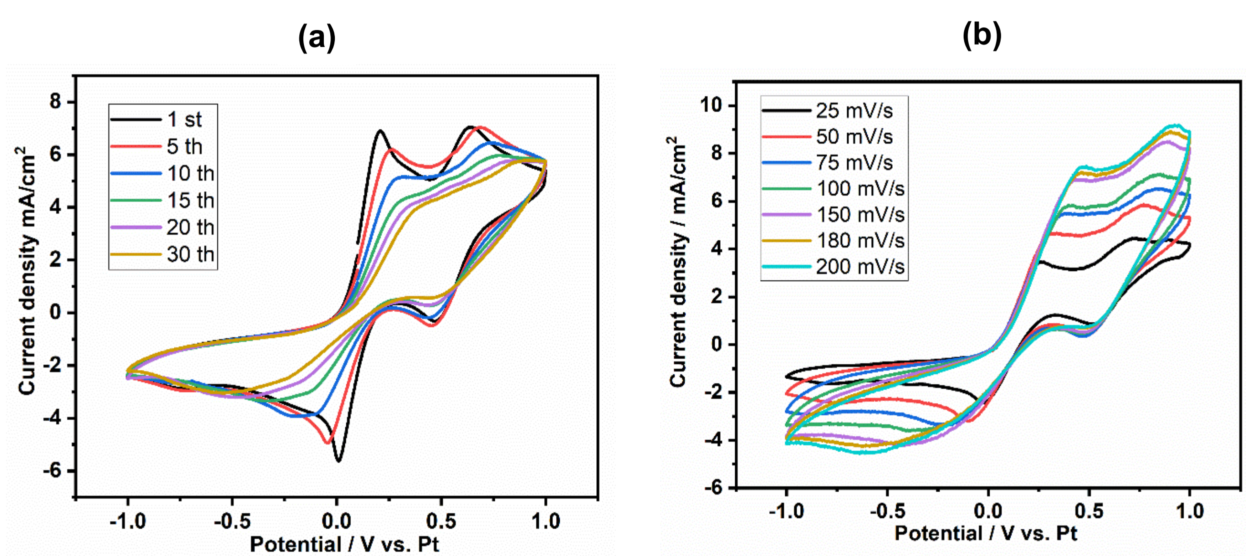

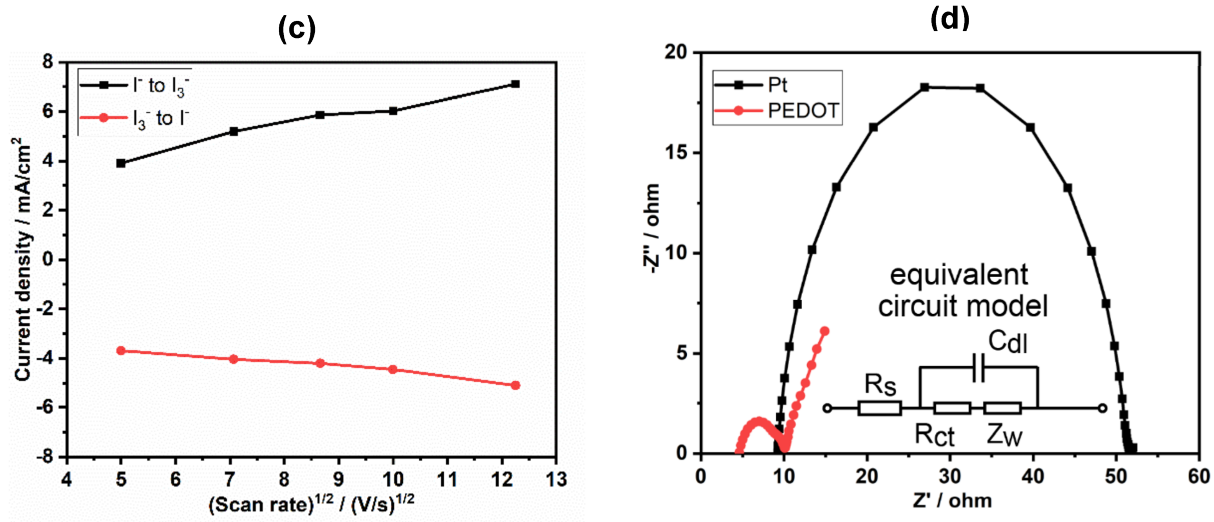

Fig. 4. Cyclic voltammograms of Pt and PEDOT film (a) at a fixed scan rate of 50 mV/s for 30 cycles; (b) at different scan rates (from inner to outer: 25, 50, 75. . . 200 mV·/s); (c) redox peak current versus the square root of the scan rate, at scan rates from 25 mV/s to 200 mV/s ; (d) Nyquist plots of the symmetric CE-CE cells and the equivalent circuit models for the I^-/I_3^- reaction.

The R_s value, which is mainly associated with the electrolyte solution resistance and the sheet resistance of the CE, is much lower for the PEDOT (4.3 Ω) than for Pt (9.2 Ω). The value of R_{ct} for the PEDOT film (7 Ω) is similarly six times lower than that for the Pt film (42 Ω), indicating a higher charge transfer process at the electrolyte and PEDOT CE interface. This difference can be associated with the high conductivity and catalytic activity of the PEDOT, which facilitate the transmission of the electrons across the PEDOT film/FTO interface. Therefore, we can expect higher photovoltaic performance from a DSSC using a PEDOT CE.

3.3. Photovoltaic performance of PEDOT CE in DSSC

The photovoltaic performances of DSSCs with PEDOT and Pt CEs were evaluated under ambient conditions. Fig. 5a is a schematic of the full cell, using FTO/TiO_2 as the working electrode and PEDOT as the CE. For comparison, Fig. 5b plots the photocurrent density–photovoltage (*J–V*) of DSSCs using PEDOT and Pt as CEs, and Table 1 lists their photovoltaic parameters.

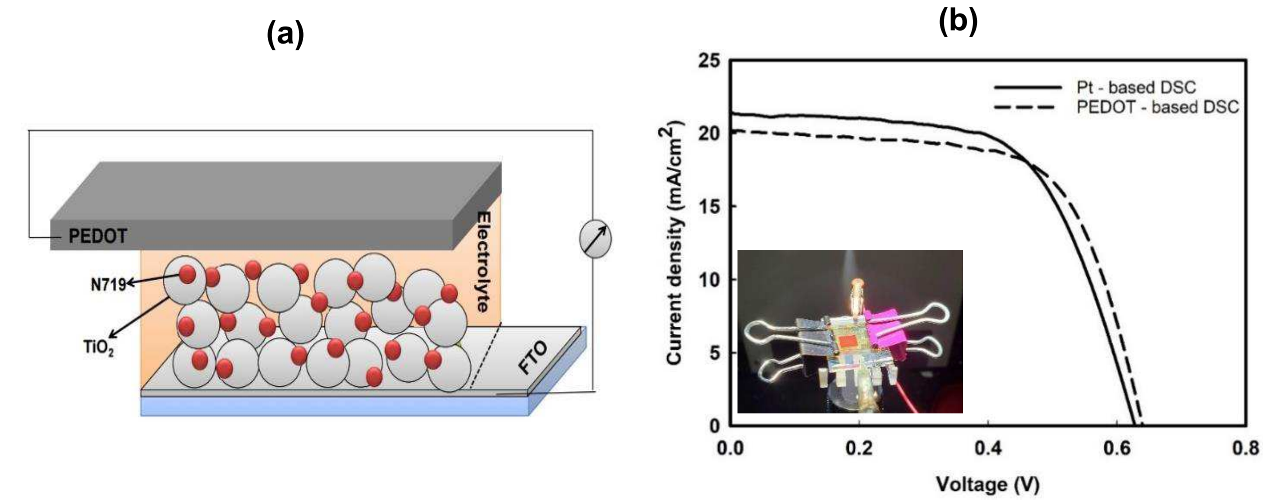

Fig. 5. (a) Schematic of a DSSC using a PEDOT film as a CE and (b) Photocurrent-voltage characteristics of DSSCs with PEDOT and Pt CEs under AM 1.5.

The open-circuit voltage (V_{OC}) values of both CEs, as listed in Table 1, are the same because we used the same TiO_2 as the working electrode for both cells. The DSSC with a PEDOT CE presents a high J_{sc} of 20.24 mA/cm^2, which is slightly lower than the Pt electrode due to the higher intrinsic electrical conductivity of the Pt. However, a higher FF value is observed for the PEDOT film, which we attribute to its low R_{ct} and excellent electrochemical catalytic activity.

Table 1. Photovoltaic parameters of the best performing DSSCs, assembled with PEDOT and Pt CEs and tested under AM 1.5.

Cell name	**J_{sc} (mA/cm^2)**	**V_{oc} (V)**	***FF* (%)**	**η (%)**
PEDOT-based DSSC	20.24	0.64	0.65	8.42
Pt-based DSSC	21.47	0.64	0.61	8.38

Moreover, the comparably high J_{sc} and *FF* values can be originated from the improved contact area between the PEDOT CE and the electrolyte (Seo et al., 1997). In general, high performance of the CE originates due to three factors, (i) the intrinsic electrocatalytic activity of CE, (ii) large contact area between the CE and the electrolyte, and (iii) the good adhesion between the CE and the substrate (Sining Yun, 2019). Here in this study, good contact area between the CE and the electrolyte can be seen from high catalytic activity of the PEDOT CE to reduce iodine to triiodide as evidence by CV analysis shown in Fig.3, while good adhesion of PEDOT to the substrate can be confirmed from Fig. 4a showing 30 successive CV of PEDOT electrode in an iodine containing electrolyte solution.

Moreover, the porous structure of the PEDOT film (Fig. 2a) can further improve the contact area between CE and electrolyte by providing more surface area for the electrolyte to react with the CE.

As a result, the PEDOT-based cell achieved an efficiency of 8.4%, among the highest of values reported in the literature, some of which are listed in Table S1. Notably, our synthesis approach is facile and cheap because we use a rust layer as the oxidant and the reaction occurs in a simple glass vial at a low temperature.

4. **Conclusions**:

Highly conductive and low-cost PEDOT films were successfully deposited on an FTO glass substrate via rust-based vapor-phase polymerization (RVPP) and used as the CE in a DSSC. CV and EIS measurements revealed a highly efficient electrochemical catalysis of the PEDOT CE, accelerating the triiodide to iodide reduction and ensuring fast electron transport at the CE/electrolyte interface. The PEDOT CE also showed a high *FF* (65%) and conversion efficiency (8.4%), slightly outperforming Pt CEs. Compared to costly and rare Pt-based CEs, the inexpensive and simple fabrication method of our PEDOT CE, in addition to its high conductivity and excellent efficiency, make it a promising candidate for large scale DSSC applications.

Acknowledgements

This work was supported by a grant from the National Science Foundation DMR-1806147. We appreciate Prof. James Ballard's editorial review of the manuscript.

REFERENCES:

Ahn, S.H., Manthiram, A., 2016. Edge-Oriented Tungsten Disulfide Catalyst Produced from Mesoporous WO $_3$ for Highly Efficient Dye-Sensitized Solar Cells. Adv. Energy Mater. 6, 1501814. https://doi.org/10.1002/aenm.201501814

Anothumakkool, B., Agrawal, I., Bhange, S.N., Soni, R., Game, O., Ogale, S.B., Kurungot, S., 2016. Pt-and TCO-Free Flexible Cathode for DSSC from Highly Conducting and Flexible PEDOT Paper Prepared via in Situ Interfacial Polymerization. Appl. Mater. interfaces 8, 553–562. https://doi.org/10.1021/acsami.5b09579

Briscoe, J., Dunn, S., 2016. The Future of Using Earth-Abundant Elements in Counter Electrodes for Dye-Sensitized Solar Cells. Adv. Mater. 28, 3802–3813. https://doi.org/10.1002/adma.201504085

Diao, Y., Chen, H., Lu, Y., Santino, L.M., Wang, H., D'arcy, J.M., 2019. Converting Rust to PEDOT Nanofibers for Supercapacitors. Appl. energy Mater. 2, 3435–3444. https://doi.org/10.1021/acsaem.9b00244

Ghani, S., Sharif, R., Bashir, S., Zaidi, A.A., Rafique, M.S., Ashraf, A., Shahzadi, S., Rafique, S., Kamboh, A.H., 2015. Polypyrrole thin films decorated with copper nanostructures as counter electrode for dye-sensitized solar cells. J. Power Sources 282, 416–420. https://doi.org/10.1016/j.jpowsour.2015.02.041

Grätzel, M., 2009. Recent advances in sensitized mesoscopic solar cells. Acc. Chem. Res. 42, 1788–1798. https://doi.org/10.1021/ar900141y

Gueye, M.N., Carella, A., Massonnet, N., Yvenou, E., Brenet, S., Jérô Me Faure-Vincent, J., Stéphanie, S., Ois Rieutord, F., Okuno, H., Benayad, A., Demadrille, R., Simonato, J.-P., 2016. Structure and Dopant Engineering in PEDOT Thin Films: Practical Tools for a Dramatic Conductivity Enhancement. https://doi.org/10.1021/acs.chemmater.6b01035

Guo, W., Zhang, X., Yu, R., Que, M., Zhang, Z., Wang, Z., Hua, Q., Wang, C., Wang, Z.L., Pan, C., 2015. CoS NWs/Au Hybridized Networks as Efficient Counter Electrodes for Flexible Sensitized Solar Cells. Adv. Energy Mater. 5, 1500141. https://doi.org/10.1002/aenm.201500141

Ha, Y.H., Nikolov, N., Pollack, S.K., Mastrangelo, J., Martin, B.D., Shashidhar, R., 2004. Towards a transparent, highly conductive poly (3,4-ethylenedioxythiophene). Adv. Funct. Mater. 14, 615–622. https://doi.org/10.1002/adfm.200305059

Han Kim, D., Atanasov, S.E., Lemaire, P., Lee, K., Parsons, G.N., 2015. Platinum-Free Cathode for Dye-Sensitized Solar Cells Using Poly(3,4-ethylenedioxythiophene) (PEDOT) Formed via Oxidative Molecular Layer Deposition. Appl. Mater. interfaces 7, 3866−3870. https://doi.org/10.1021/am5084418

Hou, W., Xiao, Y., Han, G., Lin, J.-Y., 2019. The Applications of Polymers in Solar Cells: A Review. Polymers (Basel). 11, 143. https://doi.org/10.3390/polym11010143

Jeon, S.S., Kim, C., Ko, J., Im, S.S., 2011. Spherical polypyrrole nanoparticles as a highly efficient counter electrode for dye-sensitized solar cells. J. Mater. Chem. 21, 8146–8151. https://doi.org/10.1039/c1jm10112a

Jo, S.H., Lee, Y.K., Yang, J.W., Jung, W.G., Kim, J.Y., 2012. Carbon nanotube-based flexible transparent electrode films hybridized with self-assembling PEDOT. Synth. Met. 162, 1279–1284. https://doi.org/10.1016/j.synthmet.2012.02.014

Kim, J., Kim, E., Won, Y., Lee, H., Suh, K., 2003. The preparation and characteristics of conductive poly(3,4-ethylenedioxythiophene) thin film by vapor-phase polymerization. Synth. Met. 139, 485–489. https://doi.org/10.1016/S0379-6779(03)00202-9

Kim, J., Sohn, D., Sung, Y., Kim, E.-R., n.d. Fabrication and characterization of conductive polypyrrole thin ®lm prepared by in situ vapor-phase polymerization.

Kim, J.C., Rahman, M.M., Ju, M.J., Lee, J.J., 2018. Highly conductive and stable graphene/PEDOT:PSS composite as a metal free cathode for organic dye-sensitized solar cells. RSC Adv. 8, 19058–19066. https://doi.org/10.1039/c8ra02668h

Kouhnavard, M., Ludin, N.A., Ghaffari, B.V., Ikeda, S., Sopian, K., Miyake, M., 2016. Hydrophilic carbon/TiO<inf>2</inf> colloid composite: a potential counter electrode for dye-sensitized solar cells. J. Appl. Electrochem. 46. https://doi.org/10.1007/s10800-015-0910-4

Kouhnavard, M., Ludin, N.A., Ghaffari, B.V., Ikeda, S., Sopian, K., Miyake, M., 2015. Hydrophilic carbon/TiO2 colloid composite: a potential counter electrode for dye-sensitized solar cells. J. Appl. Electrochem. 45. https://doi.org/10.1007/s10800-015-0910-4

Lee, S., Paine, D.C., Gleason, K.K., 2014a. Heavily Doped poly(3,4-ethylenedioxythiophene) Thin Films with High Carrier Mobility Deposited Using Oxidative CVD: Conductivity Stability and Carrier Transport. Adv. Funct. Mater. 24, 7178–7196. https://doi.org/10.1002/adfm.201401282

Lee, S., Paine, D.C., Gleason, K.K., 2014b. Heavily doped poly(3,4-ethylenedioxythiophene) thin films with high carrier mobility deposited using oxidative CVD: Conductivity stability and carrier transport. Adv. Funct. Mater. 24, 7187–7196. https://doi.org/10.1002/adfm.201401282

Li, Y.-C., Jia, S.-R., Liu, Z.-Y., Liu, X.-Q., Wang, Y., Cao, Y., Hu, X.-Q., Peng, C.-L., Li, Z., 2017. Fabrication of PEDOT films via a facile method and their application in Pt-free dye-sensitized solar cells †. J. Chem. A 5, 7862. https://doi.org/10.1039/c7ta00990a

Lin, Y.-F., Li, C.-T., Ho, K.-C., 2016. A template-free synthesis of the hierarchical hydroxymethyl PEDOT tube-coral array and its application in dye-sensitized solar cells †. J. Mater. Chem. A, 4, 384–394. https://doi.org/10.1039/c5ta06376k

Liu, X., Wang, M., Wang, F., Xu, T., Li, Y., Peng, X., Wei, H., Guan, Z., Zang, Z., 2020. High-Performance Photodetectors with X-Ray Responsivity Based on Interface Modified Perovskite Film. IEEE Electron Device Lett. 1–1. https://doi.org/10.1109/led.2020.2995165

Lu, C.-Y., Tsai, C.-H., Tsai, Y.-T., Hsu, C.-J., Chang, C.-H., Wu, C.-C., 2015. Spontaneous Formation of Nanofibrillar and Nanoporous Structures in High-Conductivity Conducting Polymers and Applications for Dye-Sensitized Solar Cells. Adv. Energy Mater. 5, 1401738. https://doi.org/10.1002/aenm.201401738

Park, J.W., Jang, J., 2016. Fabrication of graphene/free-standing nanofibrillar PEDOT/P(VDF-HFP) hybrid device for wearable and sensitive electronic skin application. Carbon N. Y. 87, 275–281. https://doi.org/10.1016/j.carbon.2015.02.039

Prigodin, V.N., Epstein, A.J., 2001. Nature of insulator-metal transition and novel mechanism of charge transport in the metallic state of highly doped electronic polymers. Synth. Met. 125, 43–53. https://doi.org/10.1016/S0379-6779(01)00510-0

Ren, H., Shao, H., Zhang, L., Guo, D., Jin, Q., Yu, R., Wang, L., Li, Y., Wang, Y., Zhao, H., Wang, D., 2015. A New Graphdiyne Nanosheet/Pt Nanoparticle-Based Counter Electrode Material with Enhanced Catalytic Activity for Dye-Sensitized Solar Cells. Adv. Energy Mater. 5, 1500296. https://doi.org/10.1002/aenm.201500296

Rudd, S., Franco-Gonzalez, J.F., Kumar Singh, S., Ullah Khan, Z., Crispin, X., Andreasen, J.W., Zozoulenko, I., Evans, D., 2018. Charge transport and structure in semimetallic polymers. J. Polym. Sci. Part B Polym. Phys. 56, 97–104. https://doi.org/10.1002/polb.24530

Saito, Y., Kitamura, T., Wada, Y., Yanagida, S., 2002. Application of poly(3,4-

ethylenedioxythiophene) to counter electrode in dye-sensitized solar cells. Chem. Lett. 1060–1061. https://doi.org/10.1246/cl.2002.1060

Seo, M., Fushimi, K., Takahashi, H., Aotsuka, K., Fujimoto, K., Konno, H., Kobayashi, K., Shimizu, K., Teranishi, D., Mater Sci Lett, J., Fujiwara, K., Takashima, F., Al-Odan, M., Smyrl, W.H., Papageorgiou, N., Maier, W.F., Grätzel, M., 1997. An Iodine/Triiodide Reduction Electrocatalyst for Aqueous and Organic Media, J. Electrochem. Soc. Electrochemical Society, Inc. Solid Films.

Shahzada, Ahmad, J.-H., Yum, Z., Xianxi, M., Grätzel, H.-J., Butt, M.K., Nazeeruddin, J.M., Ahmad, S., Yum, J.-H., Xianxi, Z., Gratzel, M., Butt, H.-J., Nazeeruddin, M.K., 2010. Dye-sensitized solar cells based on poly (3,4-ethylenedioxythiophene) counter electrode derived from ionic liquids PEDOT as counter electrode in the fabrication of cost effective dye-sensitized solar cells. J. Mater. Chem. 20, 1654–1658. https://doi.org/10.1039/b920210b

Shin, H.-J., Jeon, S.S., Im, S.S., 2011. CNT/PEDOT core/shell nanostructures as a counter electrode for dye-sensitized solar cells. Synth. Met. 161, 1284–1288. https://doi.org/10.1016/j.synthmet.2011.04.024

Sining Yun, A.H., 2019. Counter Electrodes for Dye-Sensitized and Perovskite Solar Cells (2 Vols.) - Google Books. John Wiley & Sons, 2019.

Sun, H., Luo, Y., Zhang, Y., Li, D., Yu, Z., Li, K., Meng, Q., n.d. In Situ Preparation of a Flexible Polyaniline/Carbon Composite Counter Electrode and Its Application in Dye-Sensitized Solar Cells. https://doi.org/10.1021/jp1030015

Tai, Q., Chen, B., Guo, F., Xu, S., Hu, H., Sebo, B., Zhao, X.Z., 2011. In situ prepared transparent polyaniline electrode and its application in bifacial dye-sensitized solar cells. ACS Nano 5, 3795–3799. https://doi.org/10.1021/nn200133g

Tang, Z., Wu, J., Zheng, M., Tang, Q., Liu, Q., Lin, J., Wang, J., 2012. High efficient PANI/Pt nanofiber counter electrode used in dye-sensitized solar cell. RSC Adv. 2, 4062. https://doi.org/10.1039/c2ra20180a

Trevisan, R., Döbbelin, M., Boix, P.P., Barea, E.M., Tena-Zaera, R., Mora-Seró, I., Bisquert, J., 2011. PEDOT Nanotube Arrays as High Performing Counter Electrodes for Dye Sensitized Solar Cells. Study of the Interactions Among Electrolytes and Counter Electrodes. Adv. Energy Mater. 1, 781–784. https://doi.org/10.1002/aenm.201100324

Ugur, A., Katmis, F., Li, M., Wu, L., Zhu, Y., Varanasi, K.K., Gleason, K.K., 2015. Low-

Dimensional Conduction Mechanisms in Highly Conductive and Transparent Conjugated Polymers. Adv. Mater. 27, 4604–4610. https://doi.org/10.1002/adma.201502340

Wang, H., Diao, Y., Rubin, M., Santino, L.M., Lu, Y., D'arcy, J.M., 2018. Metal Oxide-Assisted PEDOT Nanostructures via Hydrolysis-Assisted Vapor-Phase Polymerization for Energy Storage. https://doi.org/10.1021/acsanm.7b00382

Wang, M., Wang, H., Li, W., Hu, X., Sun, K., Zang, Z., 2019. Defect passivation using ultrathin PTAA layers for efficient and stable perovskite solar cells with a high fill factor and eliminated hysteresis †. https://doi.org/10.1039/c9ta08314f

Wang, M., Zang, Z., Yang, B., Hu, X., Sun, K., Sun, L., 2018. Performance improvement of perovskite solar cells through enhanced hole extraction: The role of iodide concentration gradient. Sol. Energy Mater. Sol. Cells 185, 117–123. https://doi.org/10.1016/j.solmat.2018.05.025

Wang, X., Zhang, X., Sun, L., Lee, D., Lee, S., Wang, M., Zhao, J., Shao-Horn, Y., Dincă, M., Palacios, T., Gleason, K.K., 2018. High electrical conductivity and carrier mobility in oCVD PEDOT thin films by engineered crystallization and acid treatment. Sci. Adv. 4, eaat5780. https://doi.org/10.1126/sciadv.aat5780

Wei, Q., Mukaida, M., Naitoh, Y., Ishida, T., 2013. Morphological change and mobility enhancement in PEDOT:PSS by adding co-solvents. Adv. Mater. 25, 2831–2836. https://doi.org/10.1002/adma.201205158

Wei, W., Wang, H., Hu, Y.H., 2014. A review on PEDOT-based counter electrodes for dye-sensitized solar cells. Int. J. Energy Res. 38, 1099–1111. https://doi.org/10.1002/er.3178

White, M.S., Kaltenbrunner, M., Głowacki, E.D., Gutnichenko, K., Kettlgruber, G., Graz, I., Aazou, S., Ulbricht, C., Egbe, D.A.M., Miron, M.C., Major, Z., Scharber, M.C., Sekitani, T., Someya, T., Bauer, S., Sariciftci, N.S., 2013. Ultrathin, highly flexible and stretchable PLEDs. Nat. Photonics 7, 811–816. https://doi.org/10.1038/nphoton.2013.188

Winther-Jensen, B., West, K., 2004a. Vapor-Phase Polymerization of 3,4-Ethylenedioxythiophene: A Route to Highly Conducting Polymer Surface Layers. https://doi.org/10.1021/ma049864l

Winther-Jensen, B., West, K., 2004b. Vapor-phase polymerization of 3,4-ethylenedioxythiophene: A route to highly conducting polymer surface layers. Macromolecules 37, 4538–4543. https://doi.org/10.1021/ma049864l

Wu, J., Lan, Z., Lin, J., Huang, M., Huang, Y., Fan, L., Luo, G., Lin, Y., Xie, Y., Wei, Y., 2017. Counter electrodes in dye-sensitized solar cells. Chem. Soc. Rev. https://doi.org/10.1039/c6cs00752j

Yue, G., Wang, L., Zhang, X., Wu, J., Jiang, Q., Zhang, W., Huang, M., Lin, J., 2014. Fabrication of high performance multi-walled carbon nanotubes/polypyrrole counter electrode for dye-sensitized solar cells. Energy 67, 460–467. https://doi.org/10.1016/j.energy.2014.01.058

Yue, G., Wu, J., Lin, J.Y., Xiao, Y., Tai, S.Y., Lin, J., Huang, M., Lan, Z., 2013. A counter electrode of multi-wall carbon nanotubes decorated with tungsten sulfide used in dye-sensitized solar cells. Carbon N. Y. 55, 1–9. https://doi.org/10.1016/j.carbon.2012.10.045

Yue, G.T., Wu, J.H., Xiao, Y.M., Lin, J.M., Huang, M.L., Fan, L.Q., Yao, Y., 2013. A dye-sensitized solar cell based on PEDOT: PSS counter electrode. Chinese Sci. Bull. 58, 559–566. https://doi.org/10.1007/s11434-012-5352-3

Zeng, X., Zhou, T., Leng, C., Zang, Z., Wang, M., Hu, W., Tang, X., Lu, S., Fang, L., Zhou, M., 2017. Performance improvement of perovskite solar cells by employing a CdSe quantum dot/PCBM composite as an electron transport layer †. https://doi.org/10.1039/c7ta00203c

Zhang, J., Long, H., Miralles, S.G., Bisquert, J., Fabregat-Santiago, F., Zhang, M., 2012. The combination of a polymer–carbon composite electrode with a high-absorptivity ruthenium dye achieves an efficient dye-sensitized solar cell based on a thiolate–disulfide redox couple. Phys. Chem. Chem. Phys 14, 7131–7136. https://doi.org/10.1039/c2cp40809k

Zhang, X., Chen, X., Zhang, K., Pang, S., Zhou, X., Xu, H., Dong, S., Han, P., Zhang, Z., Zhang, C., Cui, G., n.d. Transition-metal nitride nanoparticles embedded in N-doped reduced graphene oxide: superior synergistic electrocatalytic materials for the counter electrodes of dye-sensitized solar cells †. https://doi.org/10.1039/c2ta00608a

Zheng, X., Deng, J., Wang, N., Deng, D., Zhang, W.-H., Bao, X., Li, C., 2014. Podlike N-Doped Carbon Nanotubes Encapsulating FeNi Alloy Nanoparticles: High-Performance Counter Electrode Materials for Dye-Sensitized Solar Cells. Angew. Chemie Int. Ed. 53, 7023–7027. https://doi.org/10.1002/anie.201400388

Zhou, L., Yu, M., Chen, X., Nie, S., Lai, W.-Y., Su, W., Cui, Z., Huang, W., 2018. Screen-Printed Poly(3,4-Ethylenedioxythiophene):Poly(Styrenesulfonate) Grids as ITO-Free Anodes for Flexible Organic Light-Emitting Diodes. Adv. Funct. Mater. 28, 1705955.

https://doi.org/10.1002/adfm.201705955
Zhou, T., Wang, M., Zang, Z., Fang, L., 2019. Stable Dynamics Performance and High Efficiency of ABX_3 -Type Super-Alkali Perovskites First Obtained by Introducing H_5O_2 Cation. Adv. Energy Mater. 9, 1900664. https://doi.org/10.1002/aenm.201900664

Supporting Information:

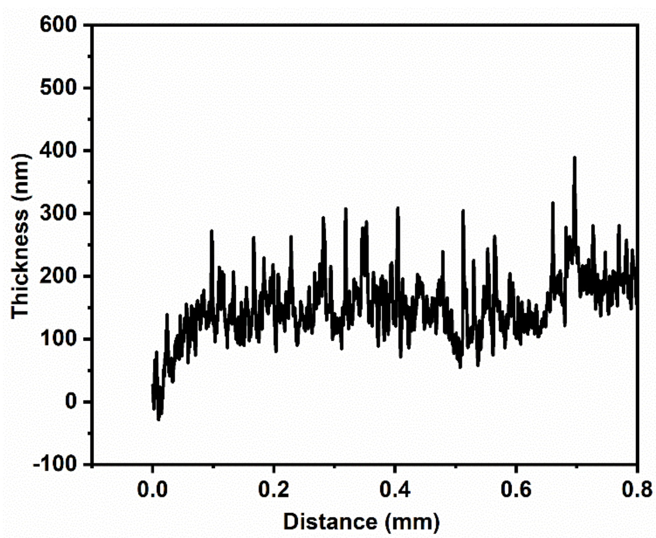

Fig. S1. Profilometer data of PEDOT thin film

Table S1. PEDOT films with different fabrication strategies, taken from the references

CE	Conductivity (S/cm)	Reaction condition	Efficiency (%)	Reference
PEDOT	**1120**	**Rust-based vapor-phase polymerization**	**8.4**	**(this work)**
PEDOT/rGO[a]	----	Potentiostat (three-electrode system) with applied voltage	7.1	(Li et al., 2017)
PEDOT	---	Oxidative molecular layer deposition using $MoCl_5$ as an oxidant	7.2	(Han Kim et al., 2015)
PEDOT	357	Humidify chamber with low pressure and gas purge system using $Fe(ClO_4)_3$ as an oxidant	6.1	(Anothumakkool et al., 2016)
PEDOT/CNT[b]	45.2	$FeCl_3$	4.62	(Shin et al., 2011)
PEDOT	195	Potentiostat (three-electrode system) with applied voltage	7.8	(Shahzada et al., 2010)
Graphene/PEDOT:PSS	6.24	Electrospray using applied voltage	8.3	(Kim et al., 2018)
Carbon +PEDOT	----	Potentiostat (three-electrode system) with applied voltage	7.6	(Zhang et al., 2012)
PEDOT:PSS	172	Scratch method under infrared light irradiation	7.6	(G. T. Yue et al., 2013)

[a]Reduced graphene oxide, [b]Single wall carbon nanotube;

*Unmarked Revised Manuscript For Publication
Click here to view linked References

Highly Conductive PEDOT Films with Enhanced Catalytic Activity for Dye-Sensitized Solar Cells

Mojgan Kouhnavard[a], Diao Yifan[b], Julio M. D' Arcy[b,c], Rohan Mishra[d], Pratim Biswas[a]*

[a]Aerosol and Air Quality Research Laboratory
Department of Energy, Environmental and Chemical Engineering
Washington University in St. Louis
One Brookings Drive
St. Louis 63130, Missouri, United States

[b]Institute of Materials Science & Engineering,
[c]Department of Chemistry
[d]Department of Mechanical Engineering & Material Science

Revised Version of SE-D-20-01655
Submitted to
Solar Energy

July 23, 2020

*To Whom Correspondence Should be Addressed: pbiswas@wustl.edu

Abstract

Low-cost poly (3,4 ethylenedioxythiophene) (PEDOT) films with a high electronic conductivity of 1021 S/cm were successfully deposited via iron oxide-based vapor-phase polymerization and used as a counter electrode (CE) in dye-sensitized solar cells for the first time. Reaching a high efficiency of 8.4%, the CE showed outstanding catalytic activity in iodine/triiodide (I^-/I_3^-) reduction, with a six times lower charge transfer resistance than a standard Pt CE. Combining low cost, easy fabrication, and high electro-catalytic activity, our PEDOT films are a promising replacement for expensive platinum CEs. This efficiency is one of the highest reported among the PEDOT-based DSSC.

Keywords: Dye-sensitized solar cell, Low-cost counter electrode, PEDOT, Vapor phase polymerization, Electrocatalytic activity, Conversion efficiency.

1. Introduction

Dye-sensitized solar cells (DSSCs) are low cost and simple to make, and they have a relatively high conversion efficiency of ~12% (Grätzel, 2009). Generally, DSSCs consist of a porous TiO_2 electrode sensitized with an absorbing layer, an electrolyte, and a platinum (Pt) counter electrode (CE). In DSSCs, CE are used to reduce an oxidized redox couple, to collect and transmit the electrons back into the cell, and to reflect unabsorbed light back to the cell, enhancing the utilization of solar energy. To ensure an efficient redox reaction in the electrolyte, an ideal CE should possess high conductivity, high electrochemical and mechanical stability, and high catalytic activity. Pt, because of its high conductivity and excellent catalytic activity toward I_3^- (iodide) reduction, is the most nearly ideal CE in DSSC (Briscoe and Dunn, 2016).

However, large-scale use of Pt is limited by its low stability in the redox electrolyte, as well as by its high cost and rarity. An alternative CE is highly desirable, one with low-cost fabrication, easy scalability, high photocorrosion stability, and relatively high conversion efficiency. To this end, many works have carried out to substitute Pt with suitable alternatives, such as carbonaceous material (Kouhnavard et al., 2016, 2015; Ren et al., 2015; Zheng et al., 2014), metal oxide (Guo et al., 2015; Ahn and Manthiram, 2016; Zhang et al., n.d.), and polymers (Ghani et al., 2015; Lu et al., 2015). Among these alternatives, polymers are advantageous for their low cost and high catalytic activity (Jeon et al., 2011; Park and Jang, 2016; Tai et al., 2011; Tang et al., 2012; Zhou et al., 2018). Polypyrrole (PPy), polyaniline (PANI) (Tai et al., 2011), and poly (3,4 ethylenedioxythiophene) (PEDOT) (Kim et al., 2018) are commonly used as conductive polymer CEs in DSSC or as hole transporting materials in perovskite solar cells (Liu et al., 2020; M. Wang et al., 2018; Wang et al., 2019; Zeng et al., 2017; Zhou et al., 2019). Amongst them, PEDOT is attractive as it possesses the highest transparency, stability, and catalytic activity (Zhang et al., 2012). Its conductivity, 300-600 $S.cm^{-1}$, is also much higher than those of PANI (~5 S/cm) and PPy (~50 S/cm) (Kim et al., n.d.; Ha et al., 2004; See et al., 2010; Wei et al., 2014;(Hou et al., 2019; Wu et al., 2017). However, the existing conductivity can be increased by various methods, such as by annealing at elevated temperatures (Lee et al., 2014a), acid treatment (Lee et al., 2014b), adding co-solvents (Wei et al., 2013; G. T. Yue et al., 2013), and doping to enhance the crystallization of the films (Gueye et al., 2016; Rudd et al., 2018). Zhang et al. used cyclic voltammetry (a three-electrode system) to deposit three different CEs with different carbon doped polymers to fabricate a DSSC (Zhang et al., 2012) with C160 ruthenium dye. PEDOT+ carbon black (C) exhibited the highest efficiency, 7.6%, compared to PANI+C and PPY+C with efficiencies of ~5.2%, prepared under the same experimental condition.

Typically, PEDOT films are generated via electrochemical polymerization under constant voltage or constant current, which results in low electrical conductivity (Trevisan et al., 2011; Lin et al., 2016; Zhang et al., 2012). For example, Li et al.(2017) report a PEDOT/rGO composite film possessing a conversion efficiency of 7.115%; however, their electrochemical method requires a potentiostat, a three-electrode system, and refined control of voltage, all of which decrease the film's reproducibility. Alternatively, toluenesulfonate, ClO, poly(styrenesulfonate) (PSS)(G. T. Yue et al., 2013), TsO ; Saito et al., 2002) and polyoxometalate (POM)) are frequently employed as dopants to increase the solubility or electrical conductivity of PEDOT. The water solubility and simple fabrication process of PEDOT:PSS make it an interesting industrial polymer. G. T. Yue et al. (2013) deposited PEDOT:PSS/carbon on an fluorine doped tin oxide (FTO) glass with a scratch method under infrared light irradiation and used it as a CE for DSSC. They achieved the highest reported conductivity for a PEDOT:PSS/carbon electrode, 173 S/cm, and a resulting cell efficiency of 7.6%.

Another synthesis approach is oxidative vapor phase polymerization (VPP) using various oxidants such as $MoCl_5$ (Han Kim et al., 2015), $Fe(ClO_4)_3$ (Anothumakkool et al., 2016), and $FeCl_3$ (Kim et al., 2003; Jo et al., 2012; X. Wang et al., 2018). However, these oxidants require fabrication in a controlled environment (Winther-Jensen and West, 2004a). Bjorn et al. synthesized a PEDOT film via chemical vapor deposition (CVD) by controlling the humidity and pressure, achieving a PEDOT conductivity of only 1000 S/cm (Winther-Jensen and West, 2004b).

It is worth noting that single-crystal PEDOT has a reported electrical conductivity as high as 8797 S/cm, which is significantly higher than that observed in the thin films desired for electronic devices (White et al., 2013). These limitations highlight the urgency of advancing current PEDOT film fabrication protocols so that they are facile, cheap, and yield high conductivity. Several methods have been proposed, mainly using VPP with $FeCl_3$ as an oxidant, but to the best of our knowledge our method has never been applied in DSSC. Herein, we present a low-cost approach for engineering superior quality PEDOT films on FTO glass, using iron oxide (rust) -based vapor-phase polymerization (RVPP) (Diao et al., 2019). We used Fe_2O_3 (rust) as an oxidant because it is the cheapest and most thermodynamically stable Fe phase. The electronic conductivity of the films are reported. The film as synthesized was used as a CE in a Pt-free DSSC.

2. Experimental:

2.1 Counter electrode preparation:

FTO glass substrates (TEC™ 7) were purchased from MSE supplies LLC, USA. First, the FTO glass substrates were washed via ultrasonic baths in acetone and then in isopropyl alcohol for 20 minutes, each. Then they were treated under UV-ozone for 30 minutes to remove remaining organic impurities.

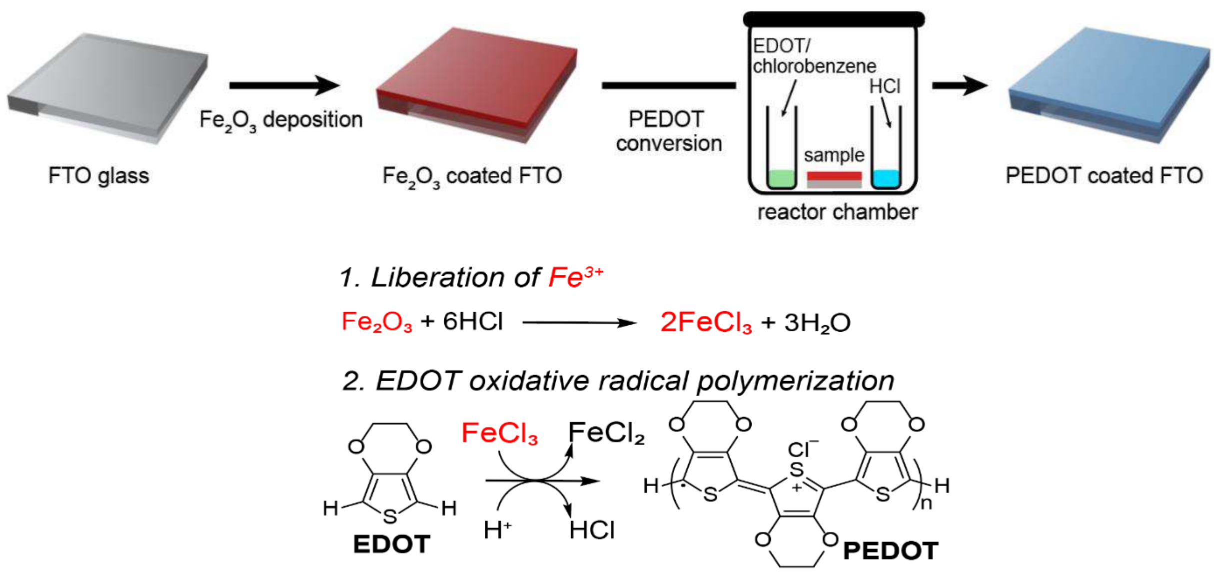

Fig. 1. Schematic of PEDOT/FTO fabrication and its mechanism for the liberation of Fe^{3+} and formation of PEDOT via step-growth polymerization.

Next, a solid-oxidant precursor, 20-nm thick Fe_2O_3, was sputtered over the FTO via physical vapor deposition (Kurt J. Lesker PVD 75 RF and DC). A glass reactor was loaded with the Fe_2O_3-coated FTO, 40 µL of HCl, and 200 µL of a 0.674 M EDOT solution in chlorobenzene, then sealed and heated in an oven at 140 °C for 1.5 hr. The samples were purified via 6 M H_2SO_4 overnight to remove iron impurities. (Fig. 1). The sputtered α-Fe_2O_3 was used as a ferric ioncontaining solid-state oxidant-precursor to induce dissolution, liberation of ferric ions, and Fe^{3+} hydrolysis concomitant with oxidative radical polymerization.

2.2 Solar cell materials and device fabrication process

A working electrode was made of two layers of screen printed TiO_2 nanoparticles (transparent TiO_2 and a reflective TiO_2) treated with $TiCl_4$, resulting in an overall thickness of 12-16 µm. The final TiO_2 film was then annealed at 450 °C for 30 minutes before immersing it in a dye solution of N719, 20 mg/mL in ethanol. The working electrode was soaked in the dye solution after being cooled to 70 °C. After 12 hours, it was rinsed with ethanol, and dried. The Pt electrode was made by drop casting Plastisol T/SP precursor solution on the FTO glass and was used as the reference CE. Finally, both the CE and the working electrode were clipped together and filled with Iodolyte AN-50 (Solaronix, Aus) electrolyte. Then the cell was tested under ambient conditions (30-50% relative humidity) and AM1.5 illumination.

2.3 Characterization:

To investigate their crystal structure, PEDOT films were characterized with an X-ray diffractometer (XRD, Bruker D8 ADVANCE, Bruker, USA) configured with a 1.5418 Å Cu X-ray operating at 40 kV. Field-emission scanning electron microscopy (FE-SEM, Nova NanoSEM 230) also used to investigate the surface morphology of the PEDOT films on the FTO substrate. Four-point probe measurements were carried out using a Keithley 2450 SourceMeter with a Signatone SP4 four-point probe head. Cyclic voltammetry (CV) analysis and electro impedance spectroscopy (EIS) were conducted using a BioLogic VMP3 multi-potentiostat. CV was carried out with three-electrode configurations at a scan rate of 50 mV/s. Ag/AgCl (3 M KCl) was used as a reference electrode, Pt and PEDOT films were the working electrodes, and Pt wire was the CE, in an acetonitrile solution containing LiI (10 mM), I_2 (1mM), and $LiClO_4$ (0.1M) as supporting electrolytes. The surface area of the CEs was 1 cm^2. EIS characterization was carried out using a symmetric cell, which consisted of two same CEs facing each other (Pt-Pt and PEDOT-PEDOT), and the space between the CEs was filled with the same electrolyte as used in full DSSC. EIS was operated at open circuit voltage using an ac perturbation of 10 mV and a frequency range 100 kHz to 0.1 Hz. The spectra were then analyzed by fitting the arc observed at the highest frequency in Nyquist plots to the equivalent circuit, which contained the series resistance (R_S), charge transfer resistance (R_{CT}), and constant phase element (CPE).

3. Results and Discussion

3.1. Morphology and crystal structure of PEDOT CE

Fig. 2a shows a SEM image of a PEDOT film on an FTO glass substrate. The film consists of bundles and nanofibers that result from, respectively, the removal of iron crystals formed during iron hydrolysis and EDOT oxidative radical polymerization through RVPP.(H. Wang et al., 2018; Diao et al., 2019). Fig. 2b shows XRD patterns of the same PEDOT film on a glass substrate. Three characteristic peaks are centered at 6.5°, 13.0°, and 26.5°. The wide diffraction peak at 26.5° corresponds to the (020) reflection, which is due to π−π stacking, whereas the sharp peaks at 6.5° and 13.0° are assigned to (200) and (100) reflections, respectively, and correspond to lateral chain packing. A four-point probe conductivity measurement was also carried out and demonstrated an exceedingly high conductivity of 1120 S/cm, mainly the result of the PEDOT crystal structure and its high charge carrier concentration (Ugur et al., 2015). The thickness of the PEDOT film is around 200 nm, measured using a profilometer (Fig. S1).

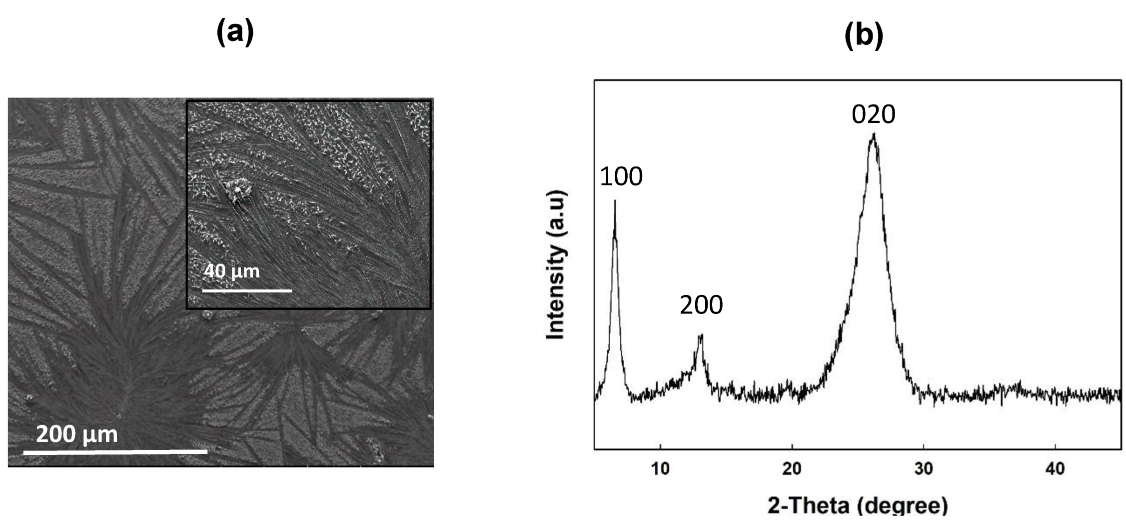

Fig. 2 (a) SEM image of a PEDOT film on an FTO substrate (b) XRD spectra of a PEDOT film on a glass substrate.

3.2. Electrochemical properties of PEDOT CE

The electrocatalytic activities of the PEDOT CEs were evaluated by CV to quantify the electrocatalytic activities of the CEs in the electrolyte. The Pt CE was also prepared under the same experimental conditions for comparison. In CV analysis, the oxidation of I^- and the reduction of I_3^- are the major redox reactions, corresponding to the anodic (J_{pa}) and cathodic (J_{pc}) peak current densities, respectively. These peaks are labeled in Fig. 3, which shows the CV diagrams of PEDOT and Pt CEs. J_{pa} in CV is not important to us, because the main role of a CE is to prompt the reduction of I_3^- in the DSSC. Therefore, J_{pc} and the potential difference between the J_{pa} and J_{pc} (ΔE_{pp}) are our focuses in this graph. The very high J_{pc} value of PEDOT (6.0 mA/cm^2), compared to Pt electrode with a J_{pc} of 2.7 mA/cm^2, indicates the outstanding electrocatalytic activity of the PEDOT CE in the I_3^- reduction reaction (Prigodin and Epstein, 2001). The lower peak potential separation (ΔE_{pp}) for PEDOT film also shows a quicker reaction rate for the reduction of I_3^- to I^-. Both factors together result in higher values of the short-current density (J_{SC}) and fill factor (FF) in a complete cell, owing to higher charge transfer through the electrolyte and CE interface and a lower recombination rate at the electrolyte and working electrode interface, respectively.

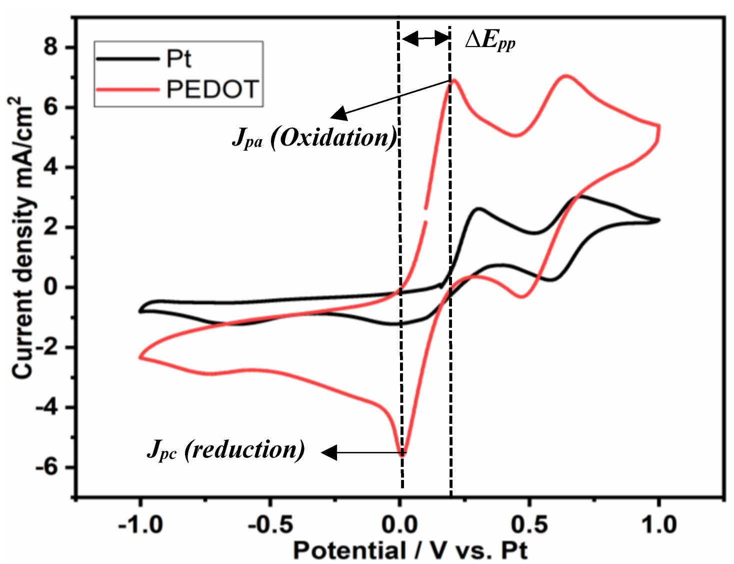

Fig. 3. Cyclic voltammograms of Pt and PEDOT film as counter electrodes for DSSC at a scan rate of 50 mV/s.

Fig. 4a shows 30 successive scan cycles of the PEDOT CE at a fixed scan rate. The peak current densities change with the change in scan rate, while the potential remains unchanged, which indicates that the PEDOT film possesses good chemical stability and is firmly coated on the FTO substrate (G. Yue et al., 2013). Fig. 4b displays the CVs of the PEDOT at scan rates ranging from 25mV/s to 200 mV/s. As the scan rate is increased, the cathodic and anodic peaks slowly shift in the negative and positive directions, respectively. In addition, Fig. 4c shows a linear relationship between the current density and the square root of the scan rate, indicating that the reduction reaction of the redox couples at the PEDOT CE is controlled by ionic diffusion of iodide species within the electrolyte, and accordingly follows the Randles-Sevcik equation (Sun et al., n.d.; Yue et al., 2014).

We further investigated the electrochemical features of the CEs by EIS measurements in a symmetric cell in which the iodine electrolyte solution was filled in the interspaces of two facing identical CEs to eliminate the effect of the photoanode. A fixed electrode area of 1 cm^2 was used for these measurements. Fig. 4d shows the Nyquist plot of the real impedance, Z’, on the x-axis versus the imaginary impedance, -Z”, on the y-axis for Pt and PEDOT cells . The intercept of the high frequency (100 kHz) semicircle on the x-axis represents the series resistance (R_s). The diameter of the high-frequency semicircle equals both the charge transfer resistance (R_{ct}) at the CE/electrolyte interface as well as the redox species (I^-/I_3^-) diffusion resistance (Z_w) in the electrolyte. The equivalent RC circuit model is also given in inset (d) of Fig. 4 and was used to obtain the EIS parameters (R_S, R_{ct}, Z_w) by fitting the impedance spectra to the equivalent model.

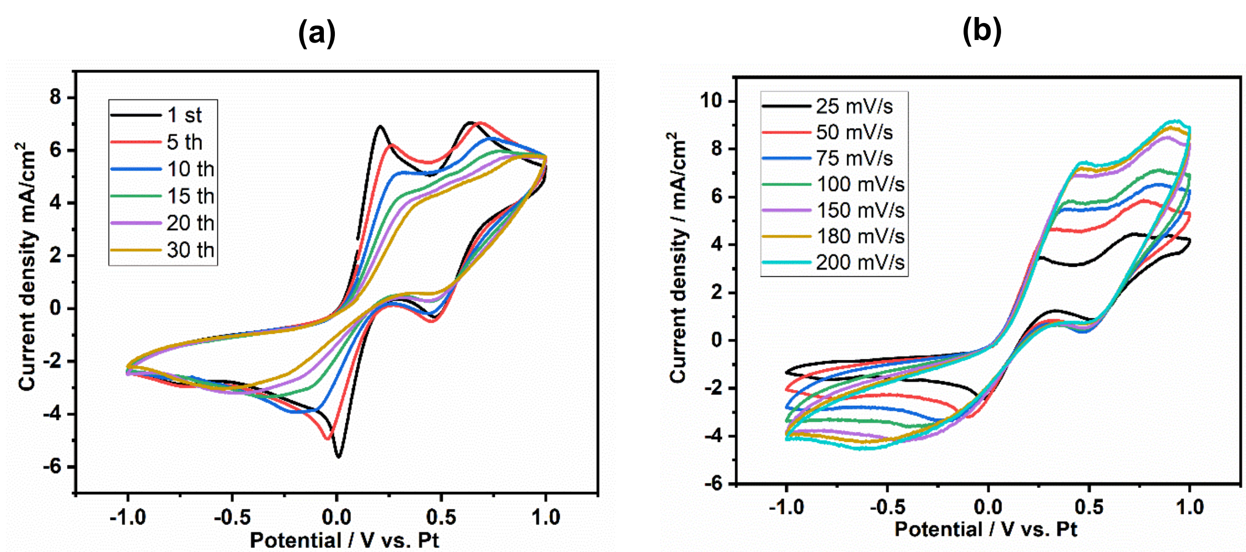

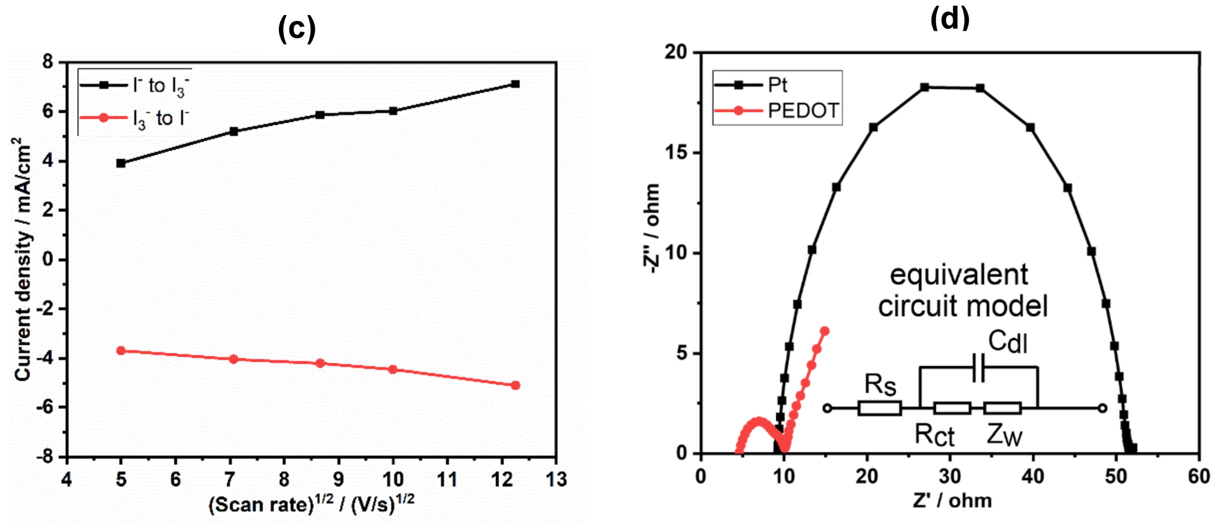

Fig. 4. Cyclic voltammograms of Pt and PEDOT film (a) at a fixed scan rate of 50 mV/s for 30 cycles; (b) at different scan rates (from inner to outer: 25, 50, 75. . . 200 mV·/s); (c) redox peak current versus the square root of the scan rate, at scan rates from 25 mV/s to 200 mV/s ; (d) Nyquist plots of the symmetric CE-CE cells and the equivalent circuit models for the I−/ I_3^- reaction.

The R_s value, which is mainly associated with the electrolyte solution resistance and the sheet resistance of the CE, is much lower for the PEDOT (4.3 Ω) than for Pt (9.2 Ω). The value of R_{ct} for the PEDOT film (7 Ω) is similarly six times lower than that for the Pt film (42 Ω), indicating a higher charge transfer process at the electrolyte and PEDOT CE interface. This difference can be associated with the high conductivity and catalytic activity of the PEDOT, which facilitate the transmission of the electrons across the PEDOT film/FTO interface. Therefore, we can expect higher photovoltaic performance from a DSSC using a PEDOT CE.

3.3. Photovoltaic performance of PEDOT CE in DSSC

The photovoltaic performances of DSSCs with PEDOT and Pt CEs were evaluated under ambient conditions. Fig. 5a is a schematic of the full cell, using FTO/TiO_2 as the working electrode and PEDOT as the CE. For comparison, Fig. 5b plots the photocurrent density–photovoltage (*J*–*V*) of DSSCs using PEDOT and Pt as CEs, and Table 1 lists their photovoltaic parameters.

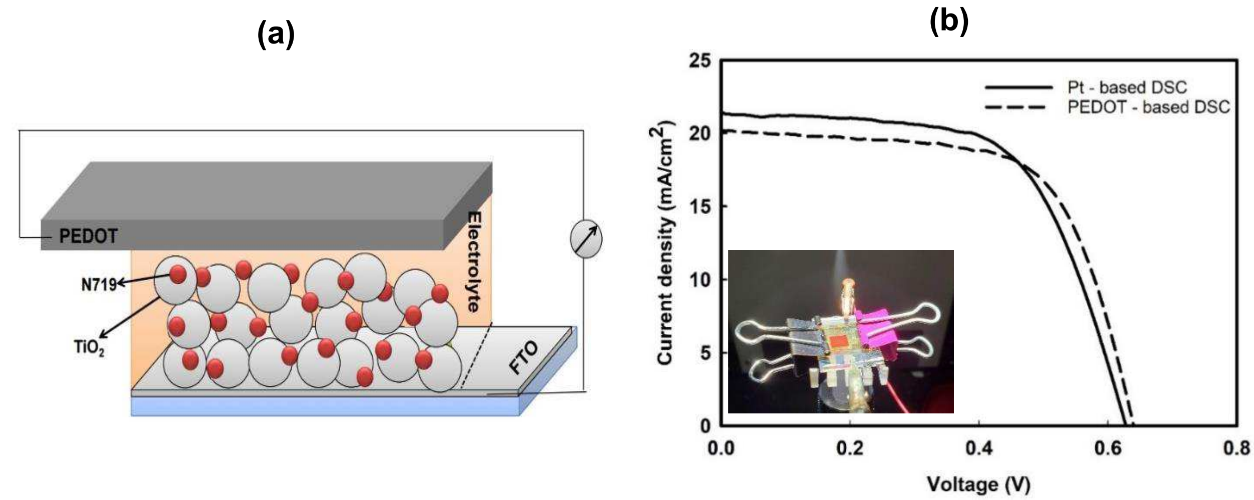

Fig. 5. (a) Schematic of a DSSC using a PEDOT film as a CE and (b) Photocurrent-voltage characteristics of DSSCs with PEDOT and Pt CEs under AM 1.5.

The open-circuit voltage (V_{OC}) values of both CEs, as listed in Table 1, are the same because we used the same TiO_2 as the working electrode for both cells. The DSSC with a PEDOT CE presents a high J_{sc} of 20.24 mA/cm^2, which is slightly lower than the Pt electrode due to the higher intrinsic electrical conductivity of the Pt. However, a higher FF value is observed for the PEDOT film, which we attribute to its low R_{ct} and excellent electrochemical catalytic activity.

Table 1. Photovoltaic parameters of the best performing DSSCs, assembled with PEDOT and Pt CEs and tested under AM 1.5.

Cell name	**J_{sc} (mA/cm^2)**	**V_{oc} (V)**	***FF* (%)**	**η (%)**
PEDOT-based DSSC	20.24	0.64	0.65	8.42
Pt-based DSSC	21.47	0.64	0.61	8.38

Moreover, the comparably high J_{sc} and *FF* values can be originated from the improved contact area between the PEDOT CE and the electrolyte (Seo et al., 1997). In general, high performance of the CE originates due to three factors, (i) the intrinsic electrocatalytic activity of CE, (ii) large contact area between the CE and the electrolyte, and (iii) the good adhesion between the CE and the substrate (Sining Yun, 2019). Here in this study, good contact area between the CE and the electrolyte can be seen from high catalytic activity of the PEDOT CE to reduce iodine to triiodide as evidence by CV analysis shown in Fig.3, while good adhesion of PEDOT to the substrate can be confirmed from Fig. 4a showing 30 successive CV of PEDOT electrode in an iodine containing electrolyte solution.

Moreover, the porous structure of the PEDOT film (Fig. 2a) can further improve the contact area between CE and electrolyte by providing more surface area for the electrolyte to react with the CE.

As a result, the PEDOT-based cell achieved an efficiency of 8.4%, among the highest of values reported in the literature, some of which are listed in Table S1. Notably, our synthesis approach is facile and cheap because we use a rust layer as the oxidant and the reaction occurs in a simple glass vial at a low temperature.

4. **Conclusions**:

Highly conductive and low-cost PEDOT films were successfully deposited on an FTO glass substrate via rust-based vapor-phase polymerization (RVPP) and used as the CE in a DSSC. CV and EIS measurements revealed a highly efficient electrochemical catalysis of the PEDOT CE, accelerating the triiodide to iodide reduction and ensuring fast electron transport at the CE/electrolyte interface. The PEDOT CE also showed a high *FF* (65%) and conversion efficiency (8.4%), slightly outperforming Pt CEs. Compared to costly and rare Pt-based CEs, the inexpensive and simple fabrication method of our PEDOT CE, in addition to its high conductivity and excellent efficiency, make it a promising candidate for large scale DSSC applications.

Acknowledgements

This work was supported by a grant from the National Science Foundation DMR-1806147. We appreciate Prof. James Ballard's editorial review of the manuscript.

REFERENCES:

Ahn, S.H., Manthiram, A., 2016. Edge-Oriented Tungsten Disulfide Catalyst Produced from Mesoporous WO $_3$ for Highly Efficient Dye-Sensitized Solar Cells. Adv. Energy Mater. 6, 1501814. https://doi.org/10.1002/aenm.201501814

Anothumakkool, B., Agrawal, I., Bhange, S.N., Soni, R., Game, O., Ogale, S.B., Kurungot, S., 2016. Pt-and TCO-Free Flexible Cathode for DSSC from Highly Conducting and Flexible PEDOT Paper Prepared via in Situ Interfacial Polymerization. Appl. Mater. interfaces 8, 553–562. https://doi.org/10.1021/acsami.5b09579

Briscoe, J., Dunn, S., 2016. The Future of Using Earth-Abundant Elements in Counter Electrodes for Dye-Sensitized Solar Cells. Adv. Mater. 28, 3802–3813. https://doi.org/10.1002/adma.201504085

Diao, Y., Chen, H., Lu, Y., Santino, L.M., Wang, H., D'arcy, J.M., 2019. Converting Rust to PEDOT Nanofibers for Supercapacitors. Appl. energy Mater. 2, 3435–3444. https://doi.org/10.1021/acsaem.9b00244

Ghani, S., Sharif, R., Bashir, S., Zaidi, A.A., Rafique, M.S., Ashraf, A., Shahzadi, S., Rafique, S., Kamboh, A.H., 2015. Polypyrrole thin films decorated with copper nanostructures as counter electrode for dye-sensitized solar cells. J. Power Sources 282, 416–420. https://doi.org/10.1016/j.jpowsour.2015.02.041

Grätzel, M., 2009. Recent advances in sensitized mesoscopic solar cells. Acc. Chem. Res. 42, 1788–1798. https://doi.org/10.1021/ar900141y

Gueye, M.N., Carella, A., Massonnet, N., Yvenou, E., Brenet, S., Jérô Me Faure-Vincent, J., Stéphanie, S., Ois Rieutord, F., Okuno, H., Benayad, A., Demadrille, R., Simonato, J.-P., 2016. Structure and Dopant Engineering in PEDOT Thin Films: Practical Tools for a Dramatic Conductivity Enhancement. https://doi.org/10.1021/acs.chemmater.6b01035

Guo, W., Zhang, X., Yu, R., Que, M., Zhang, Z., Wang, Z., Hua, Q., Wang, C., Wang, Z.L., Pan, C., 2015. CoS NWs/Au Hybridized Networks as Efficient Counter Electrodes for Flexible Sensitized Solar Cells. Adv. Energy Mater. 5, 1500141. https://doi.org/10.1002/aenm.201500141

Ha, Y.H., Nikolov, N., Pollack, S.K., Mastrangelo, J., Martin, B.D., Shashidhar, R., 2004. Towards a transparent, highly conductive poly (3,4-ethylenedioxythiophene). Adv. Funct. Mater. 14, 615–622. https://doi.org/10.1002/adfm.200305059

Han Kim, D., Atanasov, S.E., Lemaire, P., Lee, K., Parsons, G.N., 2015. Platinum-Free Cathode for Dye-Sensitized Solar Cells Using Poly(3,4-ethylenedioxythiophene) (PEDOT) Formed via Oxidative Molecular Layer Deposition. Appl. Mater. interfaces 7, 3866−3870. https://doi.org/10.1021/am5084418

Hou, W., Xiao, Y., Han, G., Lin, J.-Y., 2019. The Applications of Polymers in Solar Cells: A Review. Polymers (Basel). 11, 143. https://doi.org/10.3390/polym11010143

Jeon, S.S., Kim, C., Ko, J., Im, S.S., 2011. Spherical polypyrrole nanoparticles as a highly efficient counter electrode for dye-sensitized solar cells. J. Mater. Chem. 21, 8146–8151. https://doi.org/10.1039/c1jm10112a

Jo, S.H., Lee, Y.K., Yang, J.W., Jung, W.G., Kim, J.Y., 2012. Carbon nanotube-based flexible transparent electrode films hybridized with self-assembling PEDOT. Synth. Met. 162, 1279–1284. https://doi.org/10.1016/j.synthmet.2012.02.014

Kim, J., Kim, E., Won, Y., Lee, H., Suh, K., 2003. The preparation and characteristics of conductive poly(3,4-ethylenedioxythiophene) thin film by vapor-phase polymerization. Synth. Met. 139, 485–489. https://doi.org/10.1016/S0379-6779(03)00202-9

Kim, J., Sohn, D., Sung, Y., Kim, E.-R., n.d. Fabrication and characterization of conductive polypyrrole thin ®lm prepared by in situ vapor-phase polymerization.

Kim, J.C., Rahman, M.M., Ju, M.J., Lee, J.J., 2018. Highly conductive and stable graphene/PEDOT:PSS composite as a metal free cathode for organic dye-sensitized solar cells. RSC Adv. 8, 19058–19066. https://doi.org/10.1039/c8ra02668h

Kouhnavard, M., Ludin, N.A., Ghaffari, B.V., Ikeda, S., Sopian, K., Miyake, M., 2016. Hydrophilic carbon/TiO<inf>2</inf> colloid composite: a potential counter electrode for dye-sensitized solar cells. J. Appl. Electrochem. 46. https://doi.org/10.1007/s10800-015-0910-4

Kouhnavard, M., Ludin, N.A., Ghaffari, B.V., Ikeda, S., Sopian, K., Miyake, M., 2015. Hydrophilic carbon/TiO2 colloid composite: a potential counter electrode for dye-sensitized solar cells. J. Appl. Electrochem. 45. https://doi.org/10.1007/s10800-015-0910-4

Lee, S., Paine, D.C., Gleason, K.K., 2014a. Heavily Doped poly(3,4-ethylenedioxythiophene) Thin Films with High Carrier Mobility Deposited Using Oxidative CVD: Conductivity Stability and Carrier Transport. Adv. Funct. Mater. 24, 7178–7196. https://doi.org/10.1002/adfm.201401282

Lee, S., Paine, D.C., Gleason, K.K., 2014b. Heavily doped poly(3,4-ethylenedioxythiophene) thin films with high carrier mobility deposited using oxidative CVD: Conductivity stability and carrier transport. Adv. Funct. Mater. 24, 7187–7196. https://doi.org/10.1002/adfm.201401282

Li, Y.-C., Jia, S.-R., Liu, Z.-Y., Liu, X.-Q., Wang, Y., Cao, Y., Hu, X.-Q., Peng, C.-L., Li, Z., 2017. Fabrication of PEDOT films via a facile method and their application in Pt-free dye-sensitized solar cells †. J. Chem. A 5, 7862. https://doi.org/10.1039/c7ta00990a

Lin, Y.-F., Li, C.-T., Ho, K.-C., 2016. A template-free synthesis of the hierarchical hydroxymethyl PEDOT tube-coral array and its application in dye-sensitized solar cells †. J. Mater. Chem. A, 4, 384–394. https://doi.org/10.1039/c5ta06376k

Liu, X., Wang, M., Wang, F., Xu, T., Li, Y., Peng, X., Wei, H., Guan, Z., Zang, Z., 2020. High-Performance Photodetectors with X-Ray Responsivity Based on Interface Modified Perovskite Film. IEEE Electron Device Lett. 1–1. https://doi.org/10.1109/led.2020.2995165

Lu, C.-Y., Tsai, C.-H., Tsai, Y.-T., Hsu, C.-J., Chang, C.-H., Wu, C.-C., 2015. Spontaneous Formation of Nanofibrillar and Nanoporous Structures in High-Conductivity Conducting Polymers and Applications for Dye-Sensitized Solar Cells. Adv. Energy Mater. 5, 1401738. https://doi.org/10.1002/aenm.201401738

Park, J.W., Jang, J., 2016. Fabrication of graphene/free-standing nanofibrillar PEDOT/P(VDF-HFP) hybrid device for wearable and sensitive electronic skin application. Carbon N. Y. 87, 275–281. https://doi.org/10.1016/j.carbon.2015.02.039

Prigodin, V.N., Epstein, A.J., 2001. Nature of insulator-metal transition and novel mechanism of charge transport in the metallic state of highly doped electronic polymers. Synth. Met. 125, 43–53. https://doi.org/10.1016/S0379-6779(01)00510-0

Ren, H., Shao, H., Zhang, L., Guo, D., Jin, Q., Yu, R., Wang, L., Li, Y., Wang, Y., Zhao, H., Wang, D., 2015. A New Graphdiyne Nanosheet/Pt Nanoparticle-Based Counter Electrode Material with Enhanced Catalytic Activity for Dye-Sensitized Solar Cells. Adv. Energy Mater. 5, 1500296. https://doi.org/10.1002/aenm.201500296

Rudd, S., Franco-Gonzalez, J.F., Kumar Singh, S., Ullah Khan, Z., Crispin, X., Andreasen, J.W., Zozoulenko, I., Evans, D., 2018. Charge transport and structure in semimetallic polymers. J. Polym. Sci. Part B Polym. Phys. 56, 97–104. https://doi.org/10.1002/polb.24530

Saito, Y., Kitamura, T., Wada, Y., Yanagida, S., 2002. Application of poly(3,4-

ethylenedioxythiophene) to counter electrode in dye-sensitized solar cells. Chem. Lett. 1060–1061. https://doi.org/10.1246/cl.2002.1060

Seo, M., Fushimi, K., Takahashi, H., Aotsuka, K., Fujimoto, K., Konno, H., Kobayashi, K., Shimizu, K., Teranishi, D., Mater Sci Lett, J., Fujiwara, K., Takashima, F., Al-Odan, M., Smyrl, W.H., Papageorgiou, N., Maier, W.F., Grätzel, M., 1997. An Iodine/Triiodide Reduction Electrocatalyst for Aqueous and Organic Media, J. Electrochem. Soc. Electrochemical Society, Inc. Solid Films.

Shahzada, Ahmad, J.-H., Yum, Z., Xianxi, M., Grätzel, H.-J., Butt, M.K., Nazeeruddin, J.M., Ahmad, S., Yum, J.-H., Xianxi, Z., Gratzel, M., Butt, H.-J., Nazeeruddin, M.K., 2010. Dye-sensitized solar cells based on poly (3,4-ethylenedioxythiophene) counter electrode derived from ionic liquids PEDOT as counter electrode in the fabrication of cost effective dye-sensitized solar cells. J. Mater. Chem. 20, 1654–1658. https://doi.org/10.1039/b920210b

Shin, H.-J., Jeon, S.S., Im, S.S., 2011. CNT/PEDOT core/shell nanostructures as a counter electrode for dye-sensitized solar cells. Synth. Met. 161, 1284–1288. https://doi.org/10.1016/j.synthmet.2011.04.024

Sining Yun, A.H., 2019. Counter Electrodes for Dye-Sensitized and Perovskite Solar Cells (2 Vols.) - Google Books. John Wiley & Sons, 2019.

Sun, H., Luo, Y., Zhang, Y., Li, D., Yu, Z., Li, K., Meng, Q., n.d. In Situ Preparation of a Flexible Polyaniline/Carbon Composite Counter Electrode and Its Application in Dye-Sensitized Solar Cells. https://doi.org/10.1021/jp1030015

Tai, Q., Chen, B., Guo, F., Xu, S., Hu, H., Sebo, B., Zhao, X.Z., 2011. In situ prepared transparent polyaniline electrode and its application in bifacial dye-sensitized solar cells. ACS Nano 5, 3795–3799. https://doi.org/10.1021/nn200133g

Tang, Z., Wu, J., Zheng, M., Tang, Q., Liu, Q., Lin, J., Wang, J., 2012. High efficient PANI/Pt nanofiber counter electrode used in dye-sensitized solar cell. RSC Adv. 2, 4062. https://doi.org/10.1039/c2ra20180a

Trevisan, R., Döbbelin, M., Boix, P.P., Barea, E.M., Tena-Zaera, R., Mora-Seró, I., Bisquert, J., 2011. PEDOT Nanotube Arrays as High Performing Counter Electrodes for Dye Sensitized Solar Cells. Study of the Interactions Among Electrolytes and Counter Electrodes. Adv. Energy Mater. 1, 781–784. https://doi.org/10.1002/aenm.201100324

Ugur, A., Katmis, F., Li, M., Wu, L., Zhu, Y., Varanasi, K.K., Gleason, K.K., 2015. Low-

Dimensional Conduction Mechanisms in Highly Conductive and Transparent Conjugated Polymers. Adv. Mater. 27, 4604–4610. https://doi.org/10.1002/adma.201502340

Wang, H., Diao, Y., Rubin, M., Santino, L.M., Lu, Y., D'arcy, J.M., 2018. Metal Oxide-Assisted PEDOT Nanostructures via Hydrolysis-Assisted Vapor-Phase Polymerization for Energy Storage. https://doi.org/10.1021/acsanm.7b00382

Wang, M., Wang, H., Li, W., Hu, X., Sun, K., Zang, Z., 2019. Defect passivation using ultrathin PTAA layers for efficient and stable perovskite solar cells with a high fill factor and eliminated hysteresis †. https://doi.org/10.1039/c9ta08314f

Wang, M., Zang, Z., Yang, B., Hu, X., Sun, K., Sun, L., 2018. Performance improvement of perovskite solar cells through enhanced hole extraction: The role of iodide concentration gradient. Sol. Energy Mater. Sol. Cells 185, 117–123. https://doi.org/10.1016/j.solmat.2018.05.025

Wang, X., Zhang, X., Sun, L., Lee, D., Lee, S., Wang, M., Zhao, J., Shao-Horn, Y., Dincă, M., Palacios, T., Gleason, K.K., 2018. High electrical conductivity and carrier mobility in oCVD PEDOT thin films by engineered crystallization and acid treatment. Sci. Adv. 4, eaat5780. https://doi.org/10.1126/sciadv.aat5780

Wei, Q., Mukaida, M., Naitoh, Y., Ishida, T., 2013. Morphological change and mobility enhancement in PEDOT:PSS by adding co-solvents. Adv. Mater. 25, 2831–2836. https://doi.org/10.1002/adma.201205158

Wei, W., Wang, H., Hu, Y.H., 2014. A review on PEDOT-based counter electrodes for dye-sensitized solar cells. Int. J. Energy Res. 38, 1099–1111. https://doi.org/10.1002/er.3178

White, M.S., Kaltenbrunner, M., Głowacki, E.D., Gutnichenko, K., Kettlgruber, G., Graz, I., Aazou, S., Ulbricht, C., Egbe, D.A.M., Miron, M.C., Major, Z., Scharber, M.C., Sekitani, T., Someya, T., Bauer, S., Sariciftci, N.S., 2013. Ultrathin, highly flexible and stretchable PLEDs. Nat. Photonics 7, 811–816. https://doi.org/10.1038/nphoton.2013.188

Winther-Jensen, B., West, K., 2004a. Vapor-Phase Polymerization of 3,4-Ethylenedioxythiophene: A Route to Highly Conducting Polymer Surface Layers. https://doi.org/10.1021/ma049864l

Winther-Jensen, B., West, K., 2004b. Vapor-phase polymerization of 3,4-ethylenedioxythiophene: A route to highly conducting polymer surface layers. Macromolecules 37, 4538–4543. https://doi.org/10.1021/ma049864l

Wu, J., Lan, Z., Lin, J., Huang, M., Huang, Y., Fan, L., Luo, G., Lin, Y., Xie, Y., Wei, Y., 2017. Counter electrodes in dye-sensitized solar cells. Chem. Soc. Rev. https://doi.org/10.1039/c6cs00752j

Yue, G., Wang, L., Zhang, X., Wu, J., Jiang, Q., Zhang, W., Huang, M., Lin, J., 2014. Fabrication of high performance multi-walled carbon nanotubes/polypyrrole counter electrode for dye-sensitized solar cells. Energy 67, 460–467. https://doi.org/10.1016/j.energy.2014.01.058

Yue, G., Wu, J., Lin, J.Y., Xiao, Y., Tai, S.Y., Lin, J., Huang, M., Lan, Z., 2013. A counter electrode of multi-wall carbon nanotubes decorated with tungsten sulfide used in dye-sensitized solar cells. Carbon N. Y. 55, 1–9. https://doi.org/10.1016/j.carbon.2012.10.045

Yue, G.T., Wu, J.H., Xiao, Y.M., Lin, J.M., Huang, M.L., Fan, L.Q., Yao, Y., 2013. A dye-sensitized solar cell based on PEDOT: PSS counter electrode. Chinese Sci. Bull. 58, 559–566. https://doi.org/10.1007/s11434-012-5352-3

Zeng, X., Zhou, T., Leng, C., Zang, Z., Wang, M., Hu, W., Tang, X., Lu, S., Fang, L., Zhou, M., 2017. Performance improvement of perovskite solar cells by employing a CdSe quantum dot/PCBM composite as an electron transport layer †. https://doi.org/10.1039/c7ta00203c

Zhang, J., Long, H., Miralles, S.G., Bisquert, J., Fabregat-Santiago, F., Zhang, M., 2012. The combination of a polymer–carbon composite electrode with a high-absorptivity ruthenium dye achieves an efficient dye-sensitized solar cell based on a thiolate–disulfide redox couple. Phys. Chem. Chem. Phys 14, 7131–7136. https://doi.org/10.1039/c2cp40809k

Zhang, X., Chen, X., Zhang, K., Pang, S., Zhou, X., Xu, H., Dong, S., Han, P., Zhang, Z., Zhang, C., Cui, G., n.d. Transition-metal nitride nanoparticles embedded in N-doped reduced graphene oxide: superior synergistic electrocatalytic materials for the counter electrodes of dye-sensitized solar cells †. https://doi.org/10.1039/c2ta00608a

Zheng, X., Deng, J., Wang, N., Deng, D., Zhang, W.-H., Bao, X., Li, C., 2014. Podlike N-Doped Carbon Nanotubes Encapsulating FeNi Alloy Nanoparticles: High-Performance Counter Electrode Materials for Dye-Sensitized Solar Cells. Angew. Chemie Int. Ed. 53, 7023–7027. https://doi.org/10.1002/anie.201400388

Zhou, L., Yu, M., Chen, X., Nie, S., Lai, W.-Y., Su, W., Cui, Z., Huang, W., 2018. Screen-Printed Poly(3,4-Ethylenedioxythiophene):Poly(Styrenesulfonate) Grids as ITO-Free Anodes for Flexible Organic Light-Emitting Diodes. Adv. Funct. Mater. 28, 1705955.

https://doi.org/10.1002/adfm.201705955
Zhou, T., Wang, M., Zang, Z., Fang, L., 2019. Stable Dynamics Performance and High Efficiency of ABX_3 -Type Super-Alkali Perovskites First Obtained by Introducing H_5O_2 Cation. Adv. Energy Mater. 9, 1900664. https://doi.org/10.1002/aenm.201900664

Supporting Information:

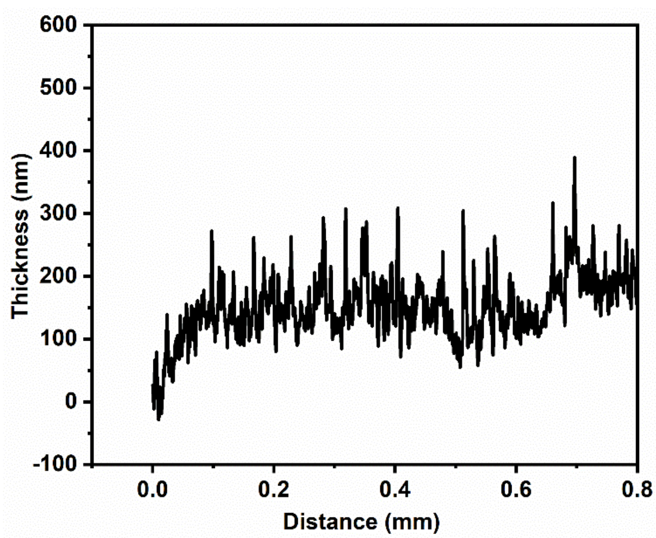

Fig. S1. Profilometer data of PEDOT thin film

Table S1. PEDOT films with different fabrication strategies, taken from the references

CE	Conductivity (S/cm)	Reaction condition	Efficiency (%)	Reference
PEDOT	**1120**	**Rust-based vapor-phase polymerization**	**8.4**	**(this work)**
PEDOT/rGO[a]	----	Potentiostat (three-electrode system) with applied voltage	7.1	(Li et al., 2017)
PEDOT	---	Oxidative molecular layer deposition using $MoCl_5$ as an oxidant	7.2	(Han Kim et al., 2015)
PEDOT	357	Humidify chamber with low pressure and gas purge system using $Fe(ClO_4)_3$ as an oxidant	6.1	(Anothumakkool et al., 2016)
PEDOT/CNT[b]	45.2	$FeCl_3$	4.62	(Shin et al., 2011)
PEDOT	195	Potentiostat (three-electrode system) with applied voltage	7.8	(Shahzada et al., 2010)
Graphene/PEDOT:PSS	6.24	Electrospray using applied voltage	8.3	(Kim et al., 2018)
Carbon +PEDOT	----	Potentiostat (three-electrode system) with applied voltage	7.6	(Zhang et al., 2012)
PEDOT:PSS	172	Scratch method under infrared light irradiation	7.6	(G. T. Yue et al., 2013)

[a]Reduced graphene oxide, [b]Single wall carbon nanotube;